REVIEW
*Biomedical Engineering Communications* 2026;5(3):14. https://doi.org/10.53388/BMEC2026014

# Biomimetic adhesives in biomedical engineering: from micro/nano structure design to applications

**Yu Gao[1], Qian Cheng[1*], Zhi-Jiang Chen[2], Feodor M. Borodich[1*], Xiao-Qing Jin[1*]**

[1]College of Aerospace Engineering, Chongqing University, Chongqing 400030, China.
[2]College of Civil Engineering, Tongji University, Shanghai 200092, China.
***Correspondence to:** Qian Cheng, College of Aerospace Engineering, Chongqing University, No. 174 Shazheng Street, Shapingba District, Chongqing 400044, China. E-mail: chengqian@cqu.edu.cn. Feodor M. Borodich, College of Aerospace Engineering, Chongqing University, No. 174 Shazheng Street, Shapingba District, Chongqing 400044, China. E-mail: borodichfm@cqu.edu.cn. Xiao-qing Jin, College of Aerospace Engineering, Chongqing University, No. 174 Shazheng Street, Shapingba District, Chongqing 400044, China. E-mail: jinxq@cqu.edu.cn.

***Author contributions***
Writing-Original Draft: Yu Gao, Qian Cheng; Revising: Yu Gao, Zhi-Jiang Chen; Funding Acquisition: Qian Cheng, Zhi-Jiang Chen, Feodor M. Borodich, Xiao-Qing Jin; Substantial Contributions To The Conception, And Final Approval Of The Version To Be Published: Feodor M. Borodich, Xiao-Qing Jin.

***Competing interests***
The authors declare no conflicts of interest.

***Acknowledgments***
This study was supported and funded by the National Natural Science Foundation of China (HWG2022001, 12402135, 52575201 and 12502114), and the China Postdoctoral Science Foundation (2024M763860). Author would also like to acknowledge the support from Chongqing City Science and Technology Program (Grant No. CSTB2025NSCQ-GPX0760, CSTB2025NSCQ-GPX0778 and CSTB2025NSCQ-GPX0784).

***Abbreviations***
JKR, Johnson-Kendall-Roberts; vdW, van der Waals; BMI, Brain-Computer Interface; ECG, Electrocardiogram; EMG, Electromyogram; mSCs, micro-Suction Cups; DBE, Degradable Biomedical Elastomers; PGA, Polyglycolic Acid; OHA, Octopus-inspired Hydrogel Adhesive; VSF, Thermo-responsive Variable Stiffness Fabric; LS-MMA, Lubricated Slippery Magnetic Responsive Microplate Array; SMMA, Superwettable Magnetic Microcilia Array; LM-MAS, Laser-Micromachined Magnetoactive Array Surfaces.

***Citation***
Gao Y, Cheng Q, Chen ZJ, Borodich FM, Jin XQ. Biomimetic adhesives in biomedical engineering: from micro/nano structure design to applications. Biomed Eng Commun. 2026;5(3):14. doi: 10.53388/BMEC2026014.

***Peer review information***
*Biomedical Engineering Communications* thanks Lin Xiao, Jian-Wei Zhang and all anonymous reviewers for their contribution to the peer review of this paper.
**Executive editor:** Jing-Wei Ma.
**Received:** 17 July 2025; **Revised**: 16 August 2025; **Accepted:** 29 September 2025; **Available online:** 10 October 2025.
© 2026 By Author(s). Published by TMR Publishing Group Limited. This is an open access article under the CC-BY license. (https://creativecommons.org/licenses/by/4.0/)

## *Abstract*
Natural evolution has endowed biological surfaces with unique microstructural features, enabling them to achieve complex functions such as grasping, climbing, and self-cleaning through precise regulation of adhesion. Inspired by this, bioinspired adhesive microstructures have shown tremendous application potential in the rapidly advancing and highly innovative biomedical field. This paper systematically reviews the adhesion systems of biological surfaces like those of geckos and tree frogs, and conducts an in-depth analysis of the adhesion mechanisms underlying various microstructures and their corresponding bioinspired adhesives from the critical perspective of structural characteristics. It reviews different types of interfacial adhesion models, with special emphasis on the suitability of the Cantor-Borodich profile model for accurately describing multiscale hierarchical adhesive structures in diverse and complex biological systems. The paper focuses on elaborating the significant contributions of bioinspired adhesives in biomedical engineering, particularly their practical and impactful applications in wearable medical devices such as stable adhesion in dynamic physiological environments, surgical instruments such as low-damage soft tissue gripping, and drug delivery systems such as enhanced transdermal delivery efficiency. Additionally, it outlines current development prospects and key challenges such as long-term biocompatibility, environmental adaptability, and structure-function synergistic optimization, providing new ideas and valuable references for further research and application of bioinspired adhesive microstructures in biomedical engineering.

**Keywords:** bioinspired adhesion; biomimetic microstructures; bioinspired adhesives; biomedical applications

*Biomedical Engineering Communications* 2026;5(3):14. https://doi.org/10.53388/BMEC2026014

## Introduction

In the rapidly evolving field of biomedical engineering, adhesive materials that integrate robust adhesion, reversible controllability, and biocompatibility have become indispensable for advancements in minimally invasive surgery, intelligent health monitoring, and precision drug delivery. Conventional adhesives often fail to meet the functional demands of dynamic physiological environments, particularly under wet conditions or on rough surfaces. Nature, however, offers ingenious solutions through organisms such as geckos, tree frogs, and octopuses, which employ hierarchical micro/nano-structured systems to achieve remarkable adhesion across diverse environments. These biological systems leverage mechanisms including van der Waals (vdW) forces, capillary action, and negative pressure, providing critical insights for designing adaptive medical adhesives.

This review systematically examines the adhesion mechanisms of biological surfaces and their translation into biomedical applications. The structural and functional principles of dry, wet, and underwater adhesion observed in geckos, tree frogs, and octopuses, respectively, are first analyzed. The hierarchical setae arrays of geckos enable reversible dry adhesion via split-contact effects [1], while tree frogs utilize hexagonal epithelial cells and capillary forces for wet adhesion [2]. Octopuses, meanwhile, rely on sucker arrays and muscle-driven negative pressure for underwater attachment [3]. Building on these adhesion principles, key interfacial adhesion models, including the Johnson-Kendall-Roberts (JKR) theory [4], Kendall peeling model [5], and capillary/suction models [6, 7], are summarized, offering a theoretical foundation for adhesive design.

Subsequently, this review provides a detailed discussion of existing engineered biomimetic adhesives, which can be categorized by structural form into setae-like (mushroom-shaped and spatula-shaped), polygonal, sucker-like, and hybrid-structured adhesives. These designs aim to replicate biological adhesion while addressing challenges like environmental adaptability, stress distribution, and fatigue resistance. Finally, the review highlights their transformative applications in medical monitoring [8, 9], soft tissue gripping [10, 11], and drug delivery [8, 12], emphasizing their potential to replace invasive procedures and enhance therapeutic precision. By bridging biological inspiration with advanced manufacturing, this work provides a roadmap for developing next-generation medical adhesives integrating environmental responsiveness, structural intelligence, and clinical practicality.

## Adhesion mechanism of biological adhesive surfaces

Over millions of years of evolution, nature has produced numerous organisms with exceptional adhesive abilities. These organisms rely on unique tissues or organs to achieve stable adhesion and friction, offering valuable insights for human research on interface adhesion behaviors. Depending on the humidity of their living environments, biological adhesion can be categorized into dry adhesion, wet adhesion, and underwater adhesion.

### Geckos (dry adhesion)

Dry adhesion is a phenomenon that enables adhesion without the assistance of liquid media, relying exclusively on interactions between microscopic surface structures of solids and intermolecular forces. Gecko adhesion is a typical example of dry adhesion. In nature, the gecko's foot has a unique microstructure, consisting of millions of tiny hair-like setae, as shown in Figure 1 [13].

The tips of these setae have further evolved into scraper-like nanostructures, with a width of approximately 200 nm and a thickness of 5 nm. Together with the setae, they form a hierarchical micro-nano structure. This micro-nano structure generates strong adhesion upon contact with solid surfaces, with the resulting adhesive force reaching several times the gecko's body weight. Autumn et al. characterized the adhesive forces of individual setae and the entire footpad, demonstrating that the primary adhesive force originates from vdW forces [14]. The vdW forces are long-range intermolecular interactions, comprising three types: induction force, orientation force, and dispersion force. Among these, the dispersion force is the main component of the total vdW force between atoms and molecules, and vdW forces are generally referred to as dispersion forces in common contexts. In biological dry adhesion systems, vdW forces play a crucial role in the total interfacial adhesive force. The dispersion force per unit area of the curved interface between two planes is expressed as follows [15]:

$$F_{vdW} = \frac{-A}{6\pi D^3} \tag{1}$$

where $A$ is the Hamaker constant and $D$ is the distance between the two contact planes.

Eq. (1) reveals the relationship between the intermolecular dispersion force and the contact distance, which directly supports the dry adhesion properties of the gecko bristles. For instance, given the extremely small distance $D$ between the tip of an individual gecko seta and the contact surface, the dispersion force per unit area can be quantified using Eq. (1). This calculation provides a mechanistic explanation for how millions of such setae collectively generate a total adhesive force adequate to support the gecko's body weight. According to the measurement data from Autumn et al. [14], when operations such as orientation, preloading, and dragging are properly performed, a single seta can generate a shear force of 194 μN and an adhesive force of 40 μN. Theoretically, a 50 g gecko with a total of 6.5 million setae can generate a considerable force: these setae can produce approximately 1300 N of shear force, which is sufficient to support the weight of two adults. The high-strength adhesion of geckos is actually achieved through "contact splitting" [1]. When a single contact is divided into many finer contacts, the adhesive force increases significantly. Following the classification by Majumder et al. [16], the contact splitting effect can be divided into: (a) external contributions to adhesive work [17]; (b) adaptability to rough surfaces; (c) size effects caused by surface-to-volume ratios [1, 4]; (d) uniform stress distribution [18]; (e) defect control and adhesive redundancy, as shown in the Figure 2 [19]. Specifically, the gecko's toes are covered with millions of micrometer-scale setae, and each seta tip splits into hundreds of nanometer-scale spatulae, forming a hierarchical fibrous structure. Contact splitting transforms a single macroscopic contact into millions of nanoscale fibrillar contacts. This structural effect can be theoretically interpreted using Eq. (1): when a macroscopic contact is hierarchically split into nanoscale setae, the fibrillar tips can conform more intimately to the surface asperities of the substrate, minimizing the distance $D$ between the seta tips and the substrate. Consequently, the dispersion force per unit area increases exponentially. This structure converts intermolecular forces into macroscopic shear resistance by maximizing the contact area and leveraging direction-dependent adhesion, which embodies the friction enhancement effect of geckos. Gao et al. further demonstrated through contact mechanics analysis that the optimized design of gecko spatulae at the nanoscale 100–250 nm can not only achieve van der Waals forces with theoretical strength but also tolerate contact defects through size effects, thereby avoiding adhesion failure caused by stress concentration [20]. The asymmetric structure of their setae can realize reversible adhesion by regulating the pulling angle 30° for attachment / 90° for detachment, which provides a mechanical basis for the rapid switching function of bionic dry adhesives.

*Biomedical Engineering Communications* 2026;5(3):14. https://doi.org/10.53388/BMEC2026014

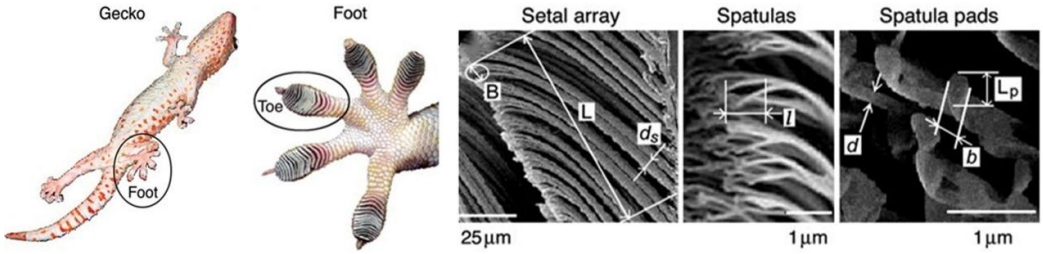



**Figure 1 The hierarchical structures of geckos.**
Reproduced with permission. Tian Y, Pesika N, Zeng H, et al. Adhesion and friction in gecko toe attachment and detachment. *Proc Natl Acad Sci USA*. 2006;103(51):19320–19325. Copyright 2006, National Academy of Sciences.

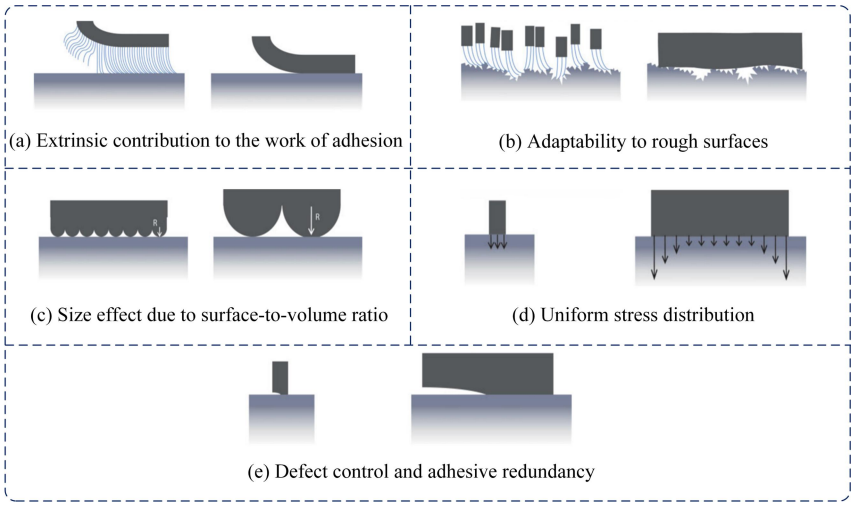



**Figure 2 Schematic diagram of "contact splitting effect" adhesion mechanisms in fibrillar surfaces.**
(a) Extrinsic contribution to the work of adhesion. (b) Adaptability to rough surfaces. (c) Size effect due to surface-to-volume ratio. (d) Uniform stress distribution. (e) Defect control and adhesive redundancy. The overall effect on adhesion may result from the superposition of some or all of these mechanisms. Reproduced with permission. Kamperman M, Kroner E, del Campo A, McMeeking RM, Arzt E. Functional Adhesive Surfaces with "Gecko" Effect: The Concept of Contact Splitting. *Adv Eng Mater*. 2010;12(5):335–348. Copyright 2010, WILEY.

In addition to geckos, other organisms have also evolved sophisticated dry adhesion mechanisms based on hierarchical structures. For instance, the adhesive setae of ladybird beetles exhibit a material gradient, with elastic modulus varying significantly from 1.2 MPa at the resilin-rich tips to 6.8 GPa at the sclerotised cuticle bases [21]. This design not only prevents setal clustering but also enhances adaptation to rough surfaces. This is an important functional requirement that aligns with the core concern of surface topography adaptation in engineering rough surface models. These models emphasize how structural features such as asperity height, distribution and mechanical properties enable interaction with uneven counter-surfaces [22]. Another typical example is spider silk anchors, which achieve robust adhesion even on anti-adhesive plant surfaces through the synergistic effect of hierarchical branching structures and discontinuous contact areas. The combination of fibrous structures and glue coatings enables effective stress distribution, avoiding premature failure.

Notably, highly efficient dry adhesion structures in nature are not limited to hair-like morphologies. Unlike the spatulate setae of geckos, the long-term adhesion systems of certain beetles and brown algae rely on mushroom-shaped microstructures. Their flattened terminal contact discs enable passive adhesion without the need for shear forces, while also possessing anti-contamination and reusability capabilities [23]. This structure optimizes interfacial stress distribution to avoid edge stress concentration, and its peeling force is twice that of smooth structures, making it particularly suitable for scenarios requiring long-term and stable adhesion.

**Tree frogs (capilary or wet adhesion)**
Under wet conditions, a liquid bridge with a meniscus form between contact surfaces, generating capillary forces and hydrodynamic forces. Capillary force arises from the surface tension of the meniscus in the liquid bridge.

Tree frogs' toe pads exhibit several notable morphological features, characterized by a specialized epidermal layer composed of multiple cell layers. The outermost layer consists of flat-topped hexagonal or cuboid columnar cells, as illustrated in Figure 3 [2, 24, 25]. The hexagonal arrangement of these cells enhances the contact area between the toe pad and diverse surfaces. This dense, regular arrangement enables the toe pad to better conform to surfaces of different shapes and textures, reducing contact gaps and thereby enhancing the stability of adhesion. Furthermore, the most prominent function of the hexagonal cells is that their arrangement forms flow-guiding channels [26]. These channels are connected to mucus glands, with the mucus secreted by the glands can reach the cell surface via these channels. This provides the necessary liquid medium for wet adhesion in tree frog toe pads, facilitating the formation of liquid bridges and capillary action to strengthen their adhesive effect.

In contrast to the wet adhesion mechanism of tree frogs, which relies on mucus-mediated liquid bridge formation, plant epicuticular wax crystals, as investigated by Borodich et al. [27, 28], exhibit anti-adhesive properties through mechanical fracture behavior. Tubular or platelet-shaped wax crystals with specific slenderness ratios undergo buckling or bending deformation under the pressure exerted by insect adhesive pads. When the applied stress exceeds their mechanical tolerance, these crystals fracture, and the fragments contaminate the adhesive pads, thereby impairing the adhesion capacity of insects. This unique anti-adhesive mechanism provides valuable insights for the design of biomedical adhesives with controllable detachment functionality.

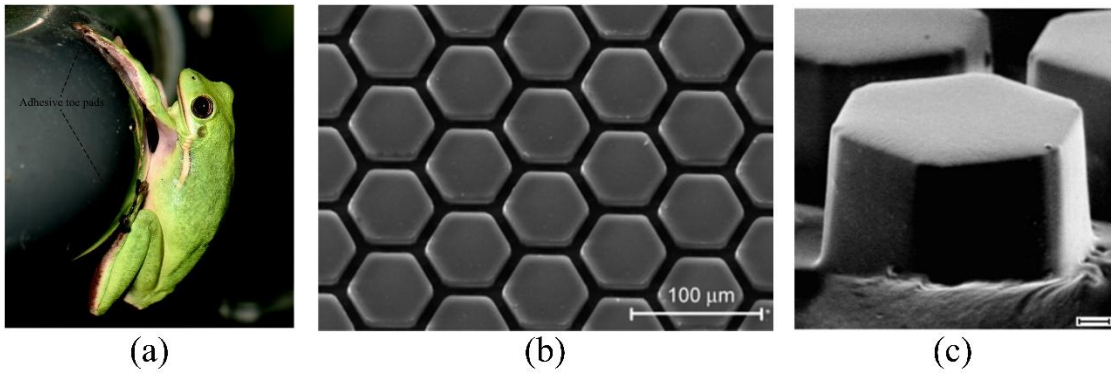



**Figure 3 Tree frog - inspired smooth adhesive surfaces.**

(a) Instances of 'smooth' adhesives inspired by tree frogs. Reproduced with permission. Langowski JKA, Dodou D, van Assenbergh P, van Leeuwen JL. Design of Tree-Frog-Inspired Adhesives. *Integr Comp Biol.* 2020;60(4):906–918. Copyright 2020, Oxford University Press. (b) Hexagonal PDMS surface patterns designed for frictional applications under dry conditions. Reproduced with permission. Murarash B, Itovich Y, Varenberg M. Tuning elastomer friction by hexagonal surface patterning. *Soft Matter*. 2011;7(12):5553–5557. Copyright 2011, Royal Society of Chemistry. (c) Hexagonally micropatterned PDMS surfaces tailored for capillary adhesion. Reproduced with permission. Drotlef D, Stepien L, Kappl M, Barnes WJP, Butt H, del Campo A. Insights into the Adhesive Mechanisms of Tree Frogs using Artificial Mimics. *Adv Funct Mater*. 2013;23(9):1137–1146. Copyright 2013, WILEY.

**Octopuses (underwater adhesion)**

In contrast to the adhesion mechanisms of geckos (dry adhesion) and tree frogs (wet adhesion), aquatic species have evolved more complex attachment systems, typically characterized by sucker-like morphological structures (Figure 4) [29]. These structures can be uniformly described using the sucker adhesion model. For instance, aquatic organisms utilize flexible suckers supported by cartilage to achieve negative pressure-based attachment [30–37], with their attachment mechanism relying on the creation of a pressure difference between the inside and outside of the sucker. The adhesive force can thus be expressed as [38]:

$$F_{\mathrm{ad}} = (p_0 - p) \cdot A \tag{2}$$

where $p_0$ and $p$ represent the external and internal pressures of the sucker, respectively, and $A$ is the contact area of the sucker. Taking the octopus as an example, the acetabular cavity within its sucker generates negative pressure through muscle contraction, while the outer edge forms a seal [3, 39, 40]. Additionally, micro-nano structures on the sucker surface contribute to consolidating the seal and enhancing friction. As a primarily underwater-dwelling organism, the octopus's negative pressure adsorption typically occurs at wet interfaces, a process closely related to the role of water in maintaining negative pressure within the cavity and at the interface. On non-wettable surfaces or in scenarios prone to cavitation, the inability of water tension to maintain the pressure difference may lead to the collapse of negative pressure-based adhesion [40–42]. However, octopuses can retain their adhesive ability out of water, owing to the multi-level fine structures on the sucker surface and muscle-driven contraction mechanisms, which enable strong adhesion across diverse interfaces [43–45]. Beyond the negative pressure adsorption mechanism, the edge folds of octopus suckers can also form liquid bridges upon contact with wet surfaces, thereby generating capillary action to enhance adsorption [44].

## Interfacial adhesion models

Based on the micro/nanostructures and adhesion models mentioned above, a better understanding of the biological adhesion mechanism can be obtained.

**Solid–solid interfacial adhesion models**

In the field of bionic microstructure design and application, the regulatory mechanism governing surface adhesion has undergone significant changes. Traditionally, such a regulatory mechanism occupied a secondary role at the macroscopic scale; however, at the micro-nano scale, it has evolved into a core element that exerts a dominant influence. As the contact size decreases, intermolecular interactions that were once deemed negligible in conventional understanding have gradually emerged as key parameters determining interfacial performance in the research on bionic surface microstructures. Notably, the theoretical underpinnings of this recognition can be traced back to the studies conducted by Derjaguin in 1934. He was the first author who pointed out that the deformation of solids should be considered when calculating the adhesive interaction between them, and made the first attempt to study the adhesion problem between elastic spheres and between an elastic sphere and an elastic half-space. He assumed that the deformation shape of the sphere could be obtained by solving the Hertz contact problem, and suggested that the adhesive interaction should be calculated by combining the attractive force between points on the solid surface and the work of adhesion, which is known as the Derjaguin approximation. Derjaguin [46] (see also Greenwood [47] and Borodich [48]) successfully derived Bradley's expression for the adhesive force $P_c$ between rigid spheres via the Derjaguin approximation (see Supplementary Eq. (S1)). As it has been mentioned, the above result is consistent with that derived by Bradley [49] via complex calculations. Subsequently, in 1964 Sperling [50] (see also [48]) adopted the Derjaguin approximation and Derjaguin's underlying concept in his discussion on the adhesion between solid particles, specifically [46]:

$$P_1 \delta a = \delta U + f_0 \delta_S \tag{3}$$

On the left-hand side, $P_1 \delta a$ represents the virtual work done by the external load $P_1$ under the virtual displacement $\delta a$. On the right-hand side, $\delta U$ denotes the virtual change in elastic deformation energy, and $f_0 \delta_S$ stands for the virtual work consumed by the increase in surface attraction. This formula expresses the physical meaning that part of the energy input by the external load is converted into the elastic deformation energy of the object, and the other part is used to overcome the surface attraction to do work. These examples fully illustrate the practicality and simplicity of the Derjaguin approximation. According to Johnson et al., and Kendall drew on Derjaguin's concepts [4, 51], equivalently treated the work done by surface attraction and the deformation work of elastic spheres, and simultaneously incorporated the stress superposition method proposed by Johnson, thereby establishing the well-known JKR adhesive contact theory. As the core theoretical framework of interfacial mechanics, the JKR adhesive contact theory plays a

fundamental role in analyzing and designing the adhesive behavior of bionic materials. By constructing a mechanical model coupling elastic solid contact with surface energy [52]. This theory provides a key tool for revealing the microscopic mechanisms of biological adhesive systems. Although the JKR theory was initially established based on the assumption of linear elastic isotropic materials, its core idea is to incorporate surface energy into the contact mechanics equilibrium equation, serving as a bridge connecting the microscopic structures of biological materials with their macroscopic adhesive properties.

The JKR model posits that the total energy $U_T$ of a contact system consists of three components Eqs. (4): the stored elastic energy $U_E$, the mechanical energy $U_M$ generated by the applied load, and the surface energy $U_S$. According to this model, the contact system reaches its actual state through two steps: first, under a specific apparent Hertzian load $P_1$, the actual contact radius $a_1$ and apparent indentation depth $\delta_1$ are generated; then, with the contact radius $a_1$ kept constant, the load is unloaded from $P_1$ to the actual value of the external load $P_0$, as detailed in Figure 5 [53].

Through derivation, the formula for the adhesive force $P$ when spheres separate in the JKR model can be obtained:

$$P = -\frac{3}{2} w \pi R_{ef} \tag{4}$$

In the formula, $w$ denotes the work of adhesion. $R_{ef}$ represents the effective radius, with its expression given by $R_I R_{II}/(R_I + R_{II})$, where $R_I$ and $R_{II}$ are the radii of curvature of the surfaces of the two contacting objects. Eq. (4) reveals the correlation between the contact force, surface energy, and elastic modulus, and serves as a core tool for analyzing dry adhesion systems such as gecko setae (see Supplementary Eqs. (S2–S10) for detailed derivation). The JKR theory is a classic model in static contact mechanics, focusing on the adhesion and elastic equilibrium during angle-free separation. This theory can explain the generation mechanism of weak adhesive forces, such as those between gecko setae and surfaces. When the setae come into contact with the surface, the elastic deformation in the contact area and the vdW forces reach equilibrium, enabling animals with setae structures to achieve stable adhesion.

JKR model has laid an important foundation for understanding adhesive contact between elastic solids. The contact mechanics framework established through energy balance methods clearly reveals the relationships between contact area, contact force, and parameters such as material surface energy and elastic modulus, providing core theoretical support for analyzing the mechanisms of biological dry adhesion systems, such as gecko setae.

However, the mechanical environment of biological systems exhibits significant particularities. Biological tissues generally display characteristics of viscoelasticity, inhomogeneity, and dynamic deformation, which are inherently different from the idealized assumptions of the JKR model, such as linear elasticity, homogeneous isotropy, and quasi-static contact. When applying the JKR model to the analysis of adhesion at biological tissue interfaces, these differences significantly limit the model's applicable boundaries. The viscoelasticity of biological tissues causes their mechanical responses to depend on time and loading rate; the inhomogeneous hierarchical structure leads to asymmetric distribution of contact stress; and dynamic processes in physiological environments, such as sliding, peeling, and cyclic loading, are difficult to be covered by the static JKR model. These constraints do not negate the theoretical value of the model but suggest that when applying the model in biomedical scenarios, full consideration should be given to the influence of actual biomechanical properties, providing a necessary premise for subsequent model analyses that are more consistent with the dynamic processes of biological adhesion.

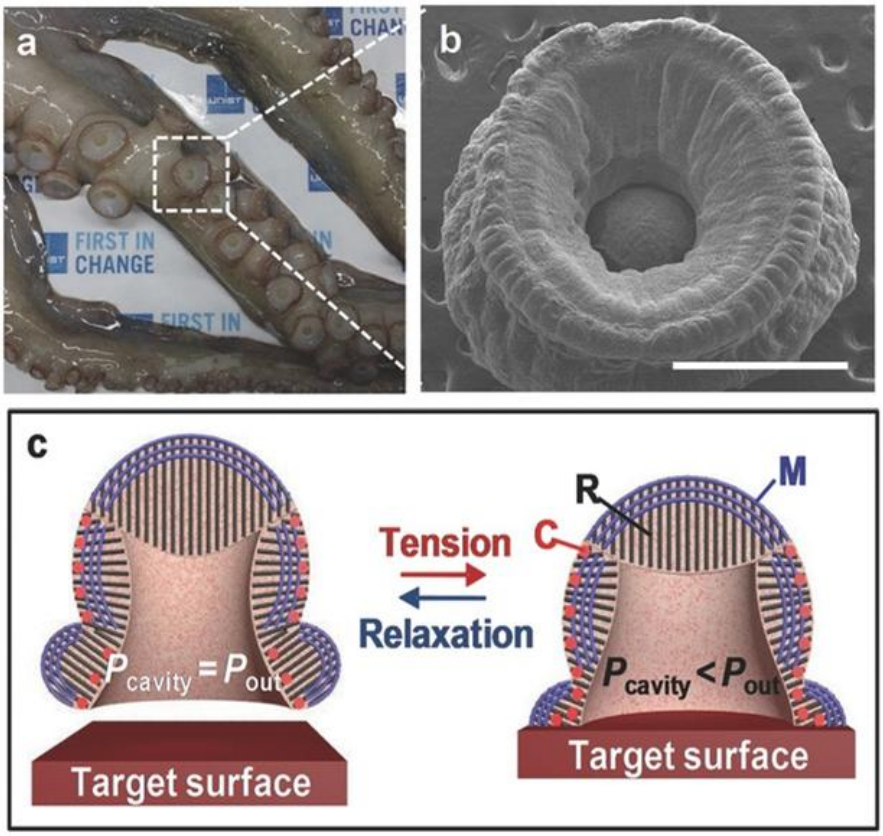



**Figure 4 Smart adhesive pads inspired by octopuses.**
(a) A photograph showing an octopus tentacle with suckers. (b) a magnified SEM image of an octopus sucker (scale bar: 1 mm). (c) a schematic diagram illustrating the adhesion process of an octopus sucker. Reproduced with permission. Lee H, Um D, Lee Y, Lim S, Kim H, Ko H. Octopus-Inspired Smart Adhesive Pads for Transfer Printing of Semiconducting Nanomembranes. *Adv Mater*. 2016;28(34):7457–7465. Copyright 2016, WILEY.

In biological adhesion systems, the adhesive performance of nanoscale fibrillar structures (such as the spatula-shaped tips of gecko setae) not only depends on macroscopic contact mechanics models like JKR but also exhibits unique scale effects. Through studying the adhesion mechanism between a single nanofiber and a substrate, Gao and Yao, et al. proposed the theory of shape-insensitive optimal adhesion, which provides a key supplement to understanding the efficient adhesion of biological nanofibrillar structures [18]. The study points out that for a given contact area $A$, the theoretical pull-off force of a fiber is $\sigma_{th}A$ (where $\sigma_{th}$ is the theoretical strength of adhesion). Theoretically, this maximum pull-off force can be achieved by optimizing the shape of the fiber tip. However, on the macroscopic scale, such a design is extremely sensitive to small changes in shape; even a slight deviation in the tip shape can lead to stress concentration, significantly reducing the actual pull-off force. Nevertheless, when the fiber diameter is reduced to approximately 100 nm, this shape sensitivity decreases significantly, enabling "shape-insensitive optimal adhesion". This explains why organisms have evolved nanoscale fibers: stable and efficient adhesion is achieved through scale optimization without relying on high-precision shape control, providing important ideas for the design of biomimetic nanoadhesives.

With the development of bionics, inspired by the microstructures that generate adhesion on the footpads of geckos and other animals, research teams at home and abroad have developed various bionic microstructured adhesives. These adhesives basically use elastic substrate films as carriers. While ensuring adhesive strength, how to release this adhesion effect is also an issue to be considered. In 1975, Kendall pointed out through energy balance analysis that the force required to peel an elastic film from a rigid substrate depends not only on the adhesive surface energy but also on the elastic deformation term, thus proposing the Kendall peeling model, as shown in Figure 6.

The Kendall model reveals the interaction relationship among the elastic term, the potential energy term, and the surface energy term during the peeling process of an elastic thin film from a rigid substrate, as follows Eq. (5):

$$\left(\frac{F_e}{b}\right)^2 \frac{1}{2dE} + \left(\frac{F_e}{b}\right)(1-\cos\theta) - W = 0 \tag{5}$$

In the formula, $b$, $d$ and $E$ denote the width, thickness, and Young's modulus of the elastic film, respectively. $F_e$ is the constant external force applied to the film, and $\theta$ is the peeling angle. This equation indicates the interaction relationship among the elastic term $(F_e/b)^2 \cdot (1/2dE)$, the potential energy term $(F_e/b)\cdot(1-\cos\theta)$, and the surface energy term $W$, laying a theoretical foundation for the subsequent study of the peeling behavior of elastic films under different conditions (see Supplementary Eq. (S11) for detailed derivation). It also provides a theoretical basis for the painless peeling of wearable bionic medical devices and the controllable shedding of biodegradable materials.

In the field of materials science and engineering, the interaction between solid surfaces is of critical importance [48, 53–57]. The JKR model and the Kendall model are two fundamental theoretical frameworks that address the contact mechanics of solid-solid interfaces, providing essential scientific support for numerous practical applications. The JKR model focuses on the mechanics of adhesive contact, describing how micro-nano surface structures and surface energy contribute to the formation of strong yet reversible adhesion. It provides a theoretical basis for designing surfaces that can achieve robust attachment through the optimization of topographical features and interfacial energy. Conversely, the Kendall model emphasizes the mechanics of peeling behavior, revealing how elastic deformation and peeling angle influence the energy dissipation during detachment. This model offers insights into minimizing peeling energy and enabling controlled delamination by adjusting geometric and mechanical parameters. Collectively, these two models constitute the mechanical foundation for understanding biological adhesion-peeling behaviors. They provide a comprehensive theoretical framework for the design of bionic materials, medical devices, and robotic systems, spanning from the optimization of strong adhesive contact to the realization of low-energy, controlled peeling processes.

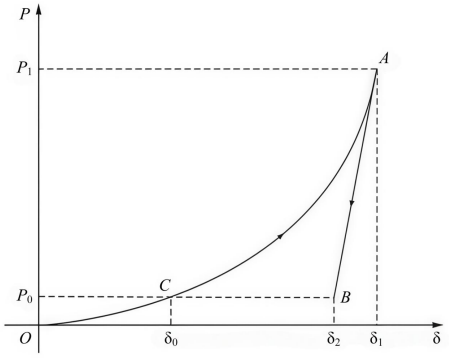



**Figure 5 Load-displacement diagram of the JKR model illustrating adhesive contact.**
In segment OA, the load-displacement curve $P-\delta$ conforms to a Hertzian $P-\delta^{(d+1)/d}$ contact relationship, whereas the relationship in segment AB is linear. Reproduced with permission. Borodich FM, Galanov BA, Suarez-Alvarez MM. The JKR-type adhesive contact problems for power-law shaped axisymmetric punches. *J Mech Phys Solids*. 2014;68:14–32. Copyright 2014, Elsevier.

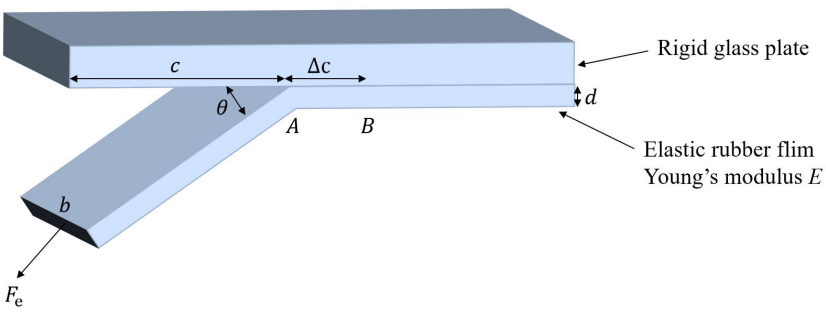



**Figure 6 Elastic film peeling from a rigid substrate (the Kendall model).**

**Solid–liquid–solid interfacial adhesion models**

Capillary force arises from the surface tension of the meniscus in a liquid bridge and is a key factor in wet contact. When a liquid meniscus forms between two wettable solid surfaces due to vapor condensation or liquid adsorption, the attractive force acting perpendicular to the surfaces is defined as the capillary force Eq. (6). It is well established that when a liquid surface exhibits a balanced curvature, a pressure difference exists between the interior and exterior of the liquid, referred to as Laplace pressure or additional pressure. Laplace pressure can be expressed as [58]:

$$\Delta p_{\mathrm{L}}=\gamma\cdot\left(\frac{1}{R_1}+\frac{1}{R_2}\right) \tag{6}$$

where $\Delta p_{\mathrm{L}}$ is the Laplace pressure, the pressure difference across the curved liquid surface, which directly contributes to the adhesive force by driving the two solid surfaces closer. $\gamma$ is the surface tension coefficient of the liquid, a critical parameter that determines the magnitude of capillary force as lower $\gamma$ facilitates easier formation of liquid bridges on biological tissues. $R_1$ is the radius of curvature of the curved liquid column, related to the width of microchannels between tree frog toe pad cells, which constrains the liquid bridge geometry. $R_2$ is the radius of curvature of the outer meniscus, dependent on the wettability of the solid surface, as shown in Figure 7a [59]. The ventral epidermis of the tree frog footpad is composed of polygonal columnar cells, with hexagonal cells accounting for the highest proportion, and a channel network 1–5 μm in width is formed between these cells [60]. The surface of the tree frog footpad is mostly covered with densely arranged hexagonal prismatic planar structures, as shown in Figure 3 [2, 24, 25]. This structure can significantly increase the wet contact area, facilitate the uniform distribution of mucus in the gap between the footpad and the substrate, and promote the rapid formation of a stable liquid bridge [60, 61]. The grooves between the columns function to drain excess liquid at the interface, while the surfaces of the columns retain a small amount of liquid to form capillary adhesion with the solid surface. The mucus secreted by the footpad forms a liquid film between the footpad and the climbing surface. When the liquid film forms a curved gas-liquid interface, Laplace pressure is generated. The total adhesive force acting on the structure has two components: one is caused by the pressure difference across the liquid-gas interface (i.e., Laplace pressure), and the other by the axial component of the liquid surface tension acting along the interface. The sum of these forces can be written as Eq. (7):

$$F_{\mathrm{ad}}=-\pi r^2\cdot\Delta p_L+2\pi r\cdot\gamma\sin\theta_1 \tag{7}$$

where $r$ is the radius of the wet area on the fiber tip, determined by the contact area between hexagonal cells and the substrate, directly affecting the magnitude of capillary force as larger $r$ increases the contact area for force transmission, and $\theta_1$ is the contact angle of the liquid with the fiber surface, ensuring strong wettability to maintain liquid bridges. The above formula describes a circular meniscus between two smooth, flat, rigid plates with equal contact angles and uniform surface energy, representing one of the most common capillary adhesion models applied to tree frog toe pads (Figure 7) [59]. However, it is known that when the tree frog is unloaded, the footpad exhibits a convex surface with a certain curvature. Therefore, the contact adhesion model between the tree frog footpad and the object surface more closely resembles a sphere-plane contact model, and the above adhesive force can be rewritten as [59]:

$$F_{\mathrm{ad}}=2\pi r\cdot\gamma\sin\theta_2\cdot\gamma\sin(\theta_1+\theta_2)-\pi r^2\gamma\left(\frac{1}{R_1}-\frac{1}{R_2}\right) \tag{8}$$

In the above formula, the filling angle $\theta_2$ is introduced, which is the angle between the vertical direction and the three-phase contact line, $\theta_2$ adjusts the effective contact area of the liquid bridge under curved surfaces. Larger $\theta_2$, meaning a more convex surface, reduces the liquid bridge stability, which tree frogs compensate for by secreting additional mucus to maintain $r$ (the expressions for $R_1$ and $R_2$ are provided in Supplementary Eq. (S13)). And $R$ is the radius of the rigid sphere, it describes the distribution of the liquid bridge on the curved surface and reflects the morphology of the liquid bridge at the footpad edge (Figure 7b) [59]. This modification bridges the gap between idealized planar models and real biological surfaces, highlighting how parameters like $R$ and $\theta_2$ correlate with the dynamic adhesion of tree frogs on rough or curved substrates. In contrast, the flat plate model only considers two-dimensional planar contact, ignoring the influence of curvature on the three-dimensional profile of the liquid bridge [6].

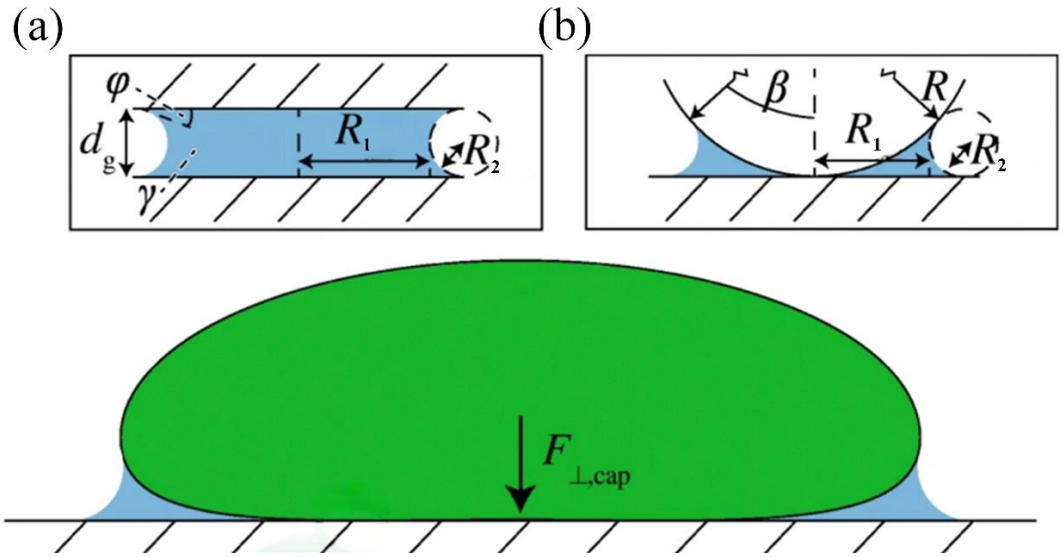



**Figure 7 Schematic diagram showing capillary adhesion between a toe pad (green) and a hydrophilic substrate, which arises from the formation of a mucus meniscus (blue).**

(a) Capillary adhesion between two flat solid plates. (b) Capillary adhesion between a solid sphere and a flat solid plate. Reproduced with permission. Langowski JKA, Dodou D, Kamperman M, van Leeuwen JL. Tree frog attachment: mechanisms, challenges, and perspectives. *Front Zool.* 2018;15:32. Copyright 2018, Springer Nature.

**Sucker model**

For organisms with sucker structures such as octopuses, their primary adhesive force originates from negative pressure adsorption. Thus, all sucker models can be interpreted through the mechanism of negative pressure adsorption. Their attachment organs rely on vacuum suckers, which achieve adsorption based on the pressure difference generated between the internal volume of the sucker and the external environment. In addition to sealing performance, the degree of vacuum of the sucker also affects the magnitude of its adsorption force. The so-called degree of vacuum of a sucker refers to the extent of the pressure difference between the interior of the sucker and the external environment when the sucker is in the adsorbed state. When suckers have the same sealing performance and size parameters, those with a higher degree of vacuum can generate greater adsorption capacity. As can be seen from the expression of Eq. (2), the form of the negative pressure formula is too simplistic to describe the adhesion behavior of octopuses. Given that the surface of octopus suckers is predominantly circular in structure, to achieve a more accurate and practical calculation of the suction adhesive force generated by octopus-inspired adhesives, the primary suction adhesive force can be expressed as follows [45]:

$$F_{ad} = \Delta p_{max} \cdot \pi r^2 \cdot n \tag{9}$$

where $\Delta p_{max}$ is the pressure difference between the inner cavity $p_{in}$ and its surrounding environment $p_{out}$, which can be expressed as $\Delta p_{max} = |p_{in} - p_{out}|$. And $\pi r^2$ is the area of a single cavity, and $n$ is the number of cavities in the adhesive patch. The above formula can explain the generation of the main adsorption force of octopus suckers and adhesives in octopus-inspired structures.

**Multiscale hierarchical models based on Cantor-Borodich ($C_B$) profile model**

The emergence of multiscale hierarchical models stems from the need to simulate the special structures of biological adhesion systems, which exhibit significant hierarchical characteristics: from macroscale such as gecko toes to microscale such as setae and nanoscale such as spatulae. Structural size decreases with hierarchy, with morphological self-similarity between levels. Such biological structures exhibit significant hierarchical characteristics: from the macroscale to the microscale, the structural size gradually decreases as the hierarchy increases, and there is morphological self-similarity between different hierarchies. This feature is highly consistent with the rough hierarchical surface model proposed by Archard [62]. By virtue of this similarity, the model cannot only describe the morphology of the adhesion system but also quantify surface roughness in the simulation of friction and adhesion contact problems [22, 63]. To achieve accurate descriptions of real geometric shapes or surface roughness in these systems, precise estimation of surface hierarchical dimensions is critical.

The complex morphology of rough surfaces serves as the starting point for research on multi-scale hierarchical models. The early Cantor-Liu profile model provided ideas for this (Figure 8a) [64]. This model is based on the Cantor bar, with a smooth base surface that evolves through generations to form a complex structure. The width of the i-th generation branch follows a specific rule, and all branches have the same height. However, it has an obvious limitation, the total height is unbounded, represented as:

$$\Delta y_0 = \Delta y_1 = \Delta y_2 = \cdots = \Delta y_i \tag{10}$$

which greatly restricts its practical application. However, this model's infinite height and uniform representative surface height limit its applicability. To overcome these limitations, Borodich established a self-similar geometric profile model identified as the $C_B$ profile based on the Cantor-Liu model (Figure 8b) [65–67]. This profile model defines scaling coefficients in the horizontal ($a_x$) and vertical ($a_z$) directions through heights ($y_i$) and widths ($x_i$) that decrease with increasing hierarchy, thereby making the total height of the $C_B$ model finite. The expressions of the scaling coefficients are as follows:

$$a_x = \frac{x_1}{x_0} = \frac{x_2}{x_1} = \cdots = \frac{x_{i+1}}{x_i}, x_{i+1} = a_x^{i+1} \cdot x_0 \tag{11a}$$

$$a_z = \frac{y_1}{y_0} = \frac{y_2}{y_1} = \ldots = \frac{y_{i+1}}{y_i} \tag{11b}$$

In fact, $a_x$ describes the ratio of width reduction between adjacent hierarchical levels. In biological systems, this parameter ensures the self-similarity of adhesive structures and increases the number of contact points with the substrate. For example, geckos have a four-level hierarchical structure. The scaling coefficient $a_x$ can be used to describe the phenomenon where each level maintains consistency while increasing the number of contact units, and amplifies van der Waals forces through the contact splitting effect. On the other hand, $a_z$ controls the ratio of height reduction between adjacent hierarchical levels, determining the overall flexibility of the structure and its ability to conform to rough surfaces. $a_z$ can describe the flexibility of gecko spatula structures to adapt to surface asperities, minimizing the distance D between contact surfaces, thereby increasing van der Waals forces (see Eq. (1)).

Combining the $C_B$ profile with spring systems represents a crucial direction for analyzing interfacial mechanical behaviors, leading to the development of various targeted models. Plesha and Ni proposed a hierarchical spring model by integrating the $C_B$ spring with the Warren and Krajcinovic models, and derived the total deflection under normal force through integrating the deformations of each spring layer (Figure 9a) [68, 69]. Schmittbuhl et al. added vertical and horizontal springs between the hierarchies of the $C_B$ profile, which not only considers lateral stiffness but also directly correlates the elastic response of the slider with interfacial friction, enabling effective analysis of the frictional characteristics of hierarchical structures (Figure 9b) [70]. Building on this, Tian et al. specifically modeled gecko setal arrays, using large springs to represent lamellae that bear the majority of normal load during preloading and provide flexible support, and small springs to represent setae that establish strong connections with the contact surface, while introducing viscous cylindrical ends to reflect adhesive forces, as shown in Figure 9c and Figure 9d [67, 71].

Beyond spring-based simulations, the Borodich-Onishchenko (B-O) profile model offers an alternative approach to constructing hierarchical structures, as illustrated in Figure 10a [72]. The $H^*$ denoted in Figure 10a represents the maximum height of this profile model, namely the maximum dimensional boundary of the entire hierarchical structure along the vertical direction. This model is characterized by a vertical scaling factor that enforces a key geometric constraint: the height of each generational block is strictly less than that of the preceding generation. Such a design ensures a controlled reduction in vertical dimensions across hierarchical levels, distinguishing it from other fractal-based models.

A defining feature of the B-O profile lies in its fractal line properties: while the total length of the fractal line is infinite, the sum of horizontal segments remains constant. The finiteness or divergence of the overall profile length is governed by a critical parameter, expressed as:

$$x^{(m)} = \begin{cases} x_0 + 2a_z x_0 \dfrac{1-(3a_z)^m}{1-3a_z} & , a_z \neq \dfrac{1}{3} \\ x_0 + 2a_z m h_0 & , a_z = \dfrac{1}{3} \end{cases} \tag{12}$$

Specifically, when the vertical scaling factor $a_z < 1/3$, the pre-structure exhibits a finite profile length, a characteristic that is closely associated with biological structures. A vivid example of this association is the octopus sucker, which features a hierarchical structure from the macroscale to the microscale. It has multi-layered folds at the edge of the sucker and micro-nano structures distributed on its surface. The $a_z$ parameter can be used to quantitatively describe the geometric characteristics of this hierarchical structure, such as the reduction ratio of different hierarchical structures in the height direction, reflecting the stability and compactness of the sucker

structure, conversely, when $a_z \geq 1/3$, the profile length tends to infinity. This parameter-dependent behavior enables the model to adapt to diverse structural scales, making it suitable for simulating complex biological adhesion systems.

Practically, the B-O profile model (see [72, 73]) has significant applications in modeling multiscale hierarchical sliders (Figure 10b) [22]. The model incorporates nanoscale elastic asperities, and their interactions are dominated by vdW forces. This enables the model to accurately capture the sliding behavior of hierarchical adhesion systems on rough surfaces. Such capability bridges the gap between microscopic interfacial forces and macroscopic frictional dynamics, providing a robust framework for analyzing adhesion-friction coupling in biological and biomimetic structures. Building on this foundation, the Borodich-Savencu hierarchical slider model was developed further and applied for nanotribology of a hierarchical model of MEMS by Almuramady et al. [22, 74].

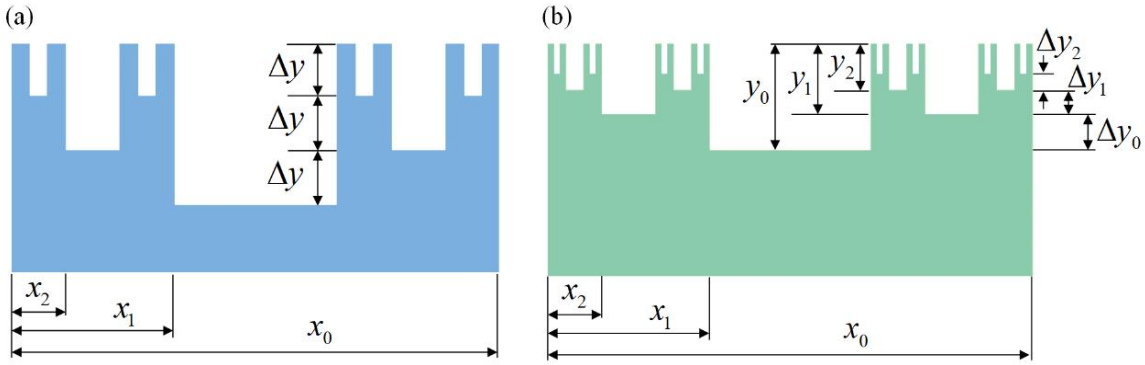



**Figure 8 Schematic illustration of surface profile models:**
(a) The Cantor-Liu profile. (b) The Cantor-Borodich profile. Reproduced with permission. Cheng Q, Borodich FM, Gao Z, Gorb SN, Jin X. Advances in the contact mechanics theory and applications of biomimetic artificial adhesives inspired by biological multiscale hierarchical structures. *Friction*. 2025;13:9441016. Copyright 2025, ScienceOpen.

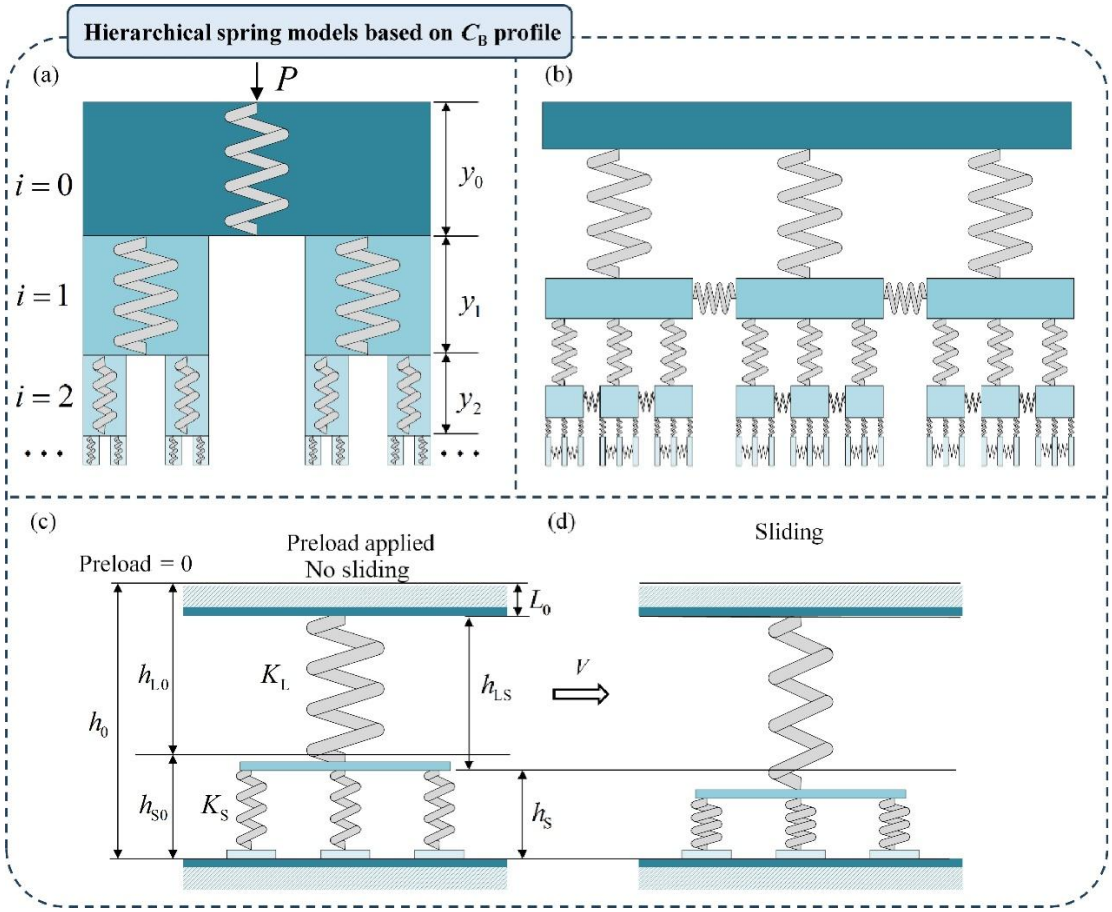



**Figure 9 Various hierarchical spring models modified from the $C_B$ profile:**
(a) The hierarchical spring model by Plesha and Ni. (b) The hierarchical model by Schmittbuhl. (c) A sketch of the perpendicular deformation in Tian's model. (d) schematic diagram of the sliding process. Reproduced with permission. Cheng Q, Borodich FM, Gao Z, Gorb SN, Jin X. Advances in the contact mechanics theory and applications of biomimetic artificial adhesives inspired by biological multiscale hierarchical structures. *Friction*. 2025;13:9441016. Copyright 2025, ScienceOpen.

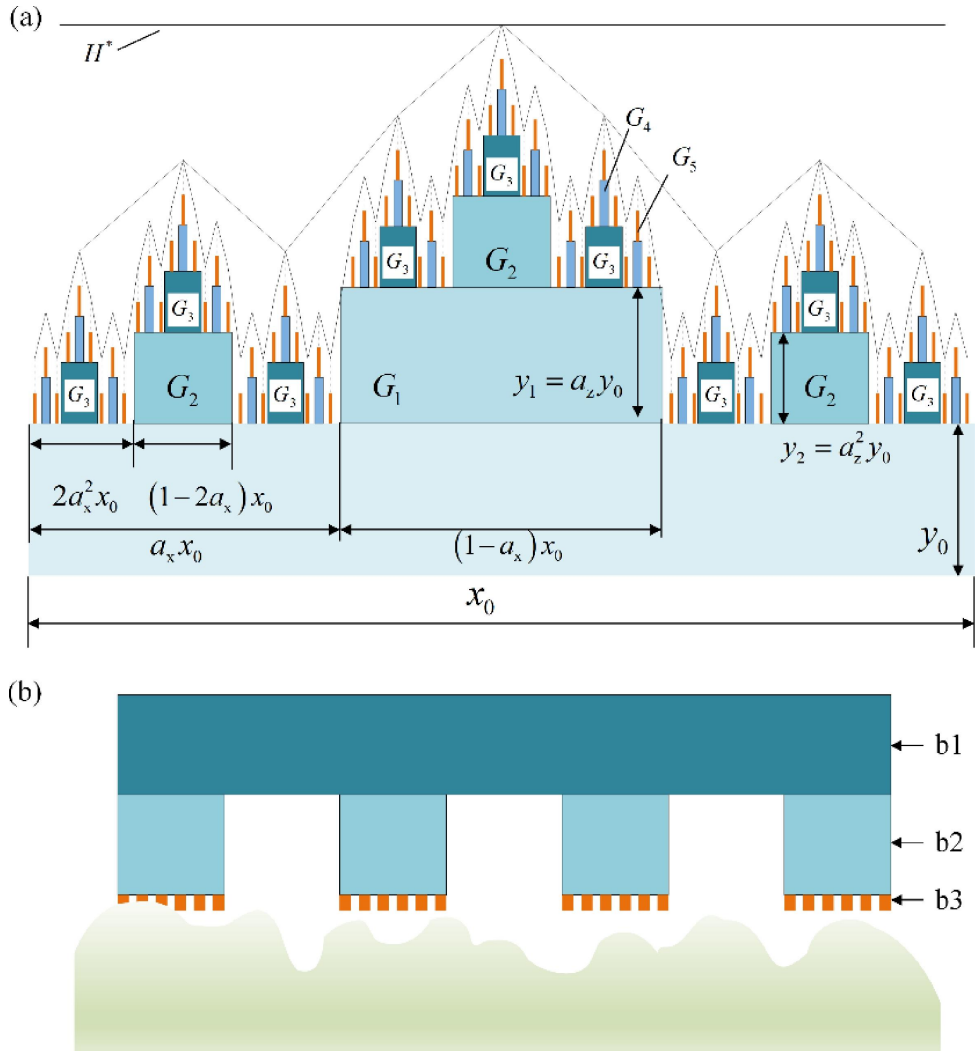



**Figure 10 Multiscale hierarchical models for rough surface adhesion and sliding.**
(a) The Borodich-Onishchenko (B-O) multilevel hierarchical model of a rough surface. (b) Multiscale, single-level, the Borodich-Savencu hierarchical slider moving along a rigid rough surface. Reproduced with permission. Cheng Q, Borodich FM, Gao Z, Gorb SN, Jin X. Advances in the contact mechanics theory and applications of biomimetic artificial adhesives inspired by biological multiscale hierarchical structures. *Friction*. 2025;13:9441016. Copyright 2025, ScienceOpen.

## Design of artificial adhesive structures

In recent decades, numerous bio-inspired artificial structural adhesives have been engineered to replicate the remarkable adhesive capabilities observed in nature, including those found in gecko pads, tree frog pads, octopus suckers, and other adhesive structures in various organisms.

### Biomimetic adhesives based on setae arrays

Gecko-inspired setae arrays serve as a prime example of dry adhesives engineered for solid–solid contact. This arrangement fosters direct interaction between two solid interfaces, triggering the generation of vdW forces resulting from molecular interactions between adjacent molecules.

As discussed earlier, geckos exhibit adhesive phenomena that are rarely observed at the macroscopic scale. Notably, animals such as geckos and spiders can adhere to walls and ceilings, and even run on vertical surfaces, by virtue of intermolecular vdW forces [75–77]. The footpads of these animals are covered with numerous hair-like adhesive setae, ranging in number from millions to billions. Each tiny seta further branches into finer setulae, with nanoscale spatula-shaped contact elements at their tips (Figure 1) [13]. These contact elements significantly influence the actual contact shape and geometry of each seta. The four-level hierarchical structure of gecko setae resolves the contradiction between “high adhesion” and “easy detachment” through multiscale coordination, a feature that dominates in some natural adhesive systems [78–80]. However, these spatula-shaped units generate adhesive force only when shear force is applied [13, 14, 81, 82], and producing shear motion requires applying counterforces in the opposite direction. To ensure normal function, therefore, the spatula elements must balance with corresponding elements acting in the opposite direction. For example, the different toes of geckos work in coordination, and some insects rely on several opposing legs to maintain shear force when moving rapidly across ceilings [77, 83–85], a process that requires muscular support. Systems based on such short-term temporary adhesion are termed active systems. When the maintenance of shear force ceases, the adhesive contact is easily broken by peeling, making these systems highly suitable for rapid movement, with connection and separation achievable within milliseconds.

In addition to the shear-force-dependent adhesive structures described above, there exists another type of structure that achieves adhesion without relying on shear force: the mushroom-shaped structure (Figure 11) [86–89]. Contact elements with a mushroom-like geometry are unaffected by applied shear force and can maintain passive adhesion without external muscular support. Combined with the requirement for relatively high breaking force to rupture the contact, these characteristics make mushroom-shaped geometries

particularly suitable for long-term attachment. For instance, in organisms inhabiting wave-swept coasts, such as many mussels [90] and for time-consuming pairing processes, as observed in scarab beetles [91, 92]. This contact element geometry has also been applied to synthetic patterned dry adhesives, where it has proven more effective than adhesive geometries using flat punch contact elements [79, 93].

The above text elaborates on two types of setal array structures: the spatula structure, which is suitable for short-term dynamic adhesion, and the mushroom structure, which is suitable for long-term passive adhesion. Taking geckos as an example, each individual contact element in the spatula structure of geckos can generate an adhesive force of approximately 10 nN [94], and multiple contact points enable successful attachment to various substrates. The spatula structure exhibits extremely low vertical detachment force but can generate strong friction under shear force, embodying the characteristic of "easy vertical detachment and strong tangential locking". This characteristic stems from the flexibility of the spatula protrusions: when a shear force is applied, the protrusions bend to increase the real contact area, whereas vertical peeling leads to rapid fracture due to stress concentration. This offers the advantage that adhesive systems designed based on the spatula structure can achieve rapid adhesion and detachment processes.

Furthermore, the study by Cheng et al. revealed that the overall stiffness of the spatula-shaped synthetic adhesive can be modulated by altering the geometry of the setae and the terminal spatula, thereby tuning its adhesive performance on rough surfaces [54]. They designed two synthetic adhesive prototypes, named Seta-I and Seta-II, respectively (Figure 12) [54]. Relying on differences in structural stiffness, these two synthetic adhesives can regulate the real contact area under normal pressure, thereby enabling strong adhesion or controllable attachment–detachment capabilities on rough surfaces.

For the mushroom-shaped array structure, one of its primary advantages lies in its ability to enhance adhesion while exhibiting multi-environmental adaptability. In dry environments, experimental results have confirmed that on a smooth glass surface, the detachment force of the mushroom-shaped structure reaches approximately 360 mN, nearly twice that of the smooth control sample (about 180 mN), and notably, this performance is achieved without relying on preloading [95]. Furthermore, comparative studies have verified that, in contrast to smooth surfaces, the mushroom-shaped structured surface displays strong tolerance to environmental contamination. Even when exposed to thick layers of dust, it retains significantly higher peel strength than smooth surfaces, highlighting its robustness in harsh conditions. In humid environments and even underwater, the mushroom-shaped structure demonstrates superior adhesion compared to its performance in dry air [96, 97]. This phenomenon can be attributed to a unique physical mechanism: when the mushroom-shaped structure traps water at the contact interface, and the glass substrate reaches the cavitation threshold, the trapped water undergoes phase transition into vapor. This phase change generates a localized suction effect, allowing each individual mushroom-shaped structure to function as a passive suction device that enhances interfacial bonding [97]. Precisely due to its combination of passive adhesion, resistance to pollution, and adaptability across diverse environments from dry and dusty conditions to humid and underwater settings, the mushroom-shaped array structure has emerged as an ideal candidate for a wide range of industrial applications, including precision manufacturing, medical device fixation, and underwater equipment bonding.

In recent years, scalable nanofabrication technologies such as roll-to-roll nanoimprinting have brought hope for the large-scale production of gecko-inspired setal array adhesives. Through a continuous imprinting process, roll-to-roll nanoimprinting technology can quickly replicate micro/nano structures on large-area flexible materials. When producing biomimetic adhesives based on setal arrays, using customized templates, this technology can accurately replicate setal structures with specific shapes and sizes. Whether it is the shovel-shaped structures suitable for short-term dynamic adhesion or the mushroom-shaped structures suitable for long-term passive adhesion, efficient production can be achieved. This not only improves production efficiency but also ensures the structural consistency of products from different batches, laying a foundation for the large-scale promotion of such biomimetic adhesives in practical applications. At the same time, combining auxiliary technologies such as in-situ plasma treatment can further optimize the adhesion and demolding performance between the template and the material, making the production process more stable and reliable. In addition, transfer printing technology provides a flexible solution for the heterogeneous integration of bionic bristle arrays. Linghu et al. demonstrated that gecko-inspired fibrillar stamps with shear-enhanced adhesion and a switching ratio greater than 100:1 can achieve precise transfer of micro-nano structures onto flexible substrates [98]. Aphid-inspired inflatable stamps adapt to the assembly requirements of complex curved surfaces through contact area regulation, significantly expanding the manufacturing feasibility of bionic adhesives in flexible electronic devices.

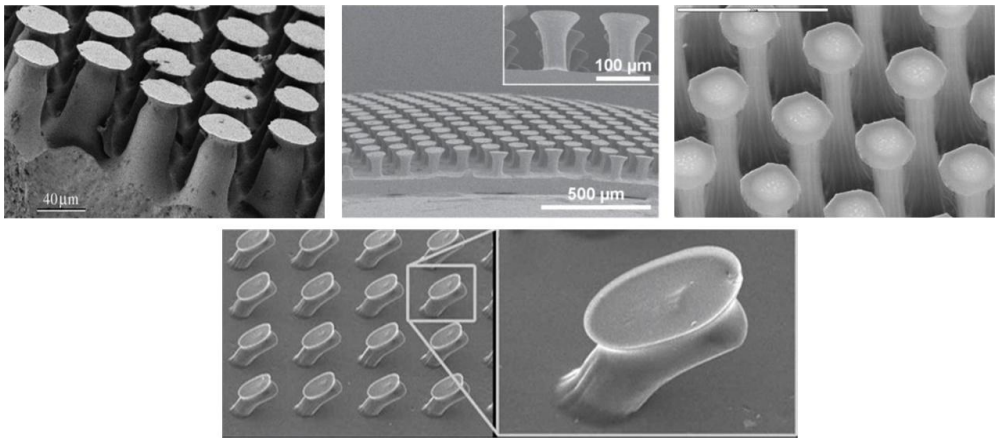



**Figure 11 SEM images of various mushroom-shaped bioinspired adhesives.**
Reproduced with permission. Carbone G, Pierro E. Sticky Bio-inspired Micropillars: Finding the Best Shape. *Small*. 2012;8(9):1449–1454. Copyright 2012, WILEY. Song S, Sitti M. Soft Grippers Using Micro-fibrillar Adhesives for Transfer Printing. *Adv Mater*. 2014;26(28):4901–4906. Copyright 2014, WILEY. Davies J, Haq S, Hawke T, Sargent JP. A practical approach to the development of a synthetic Gecko tape. *Int J Adhes Adhes*. 2009;29(4):380–390. 89. Copyright 2009, Elsevier. Murphy MP, Aksak B, Sitti M. Gecko-Inspired Directional and Controllable Adhesion. *Small*. 2009;5(2):170–175. Copyright 2009, WILEY.

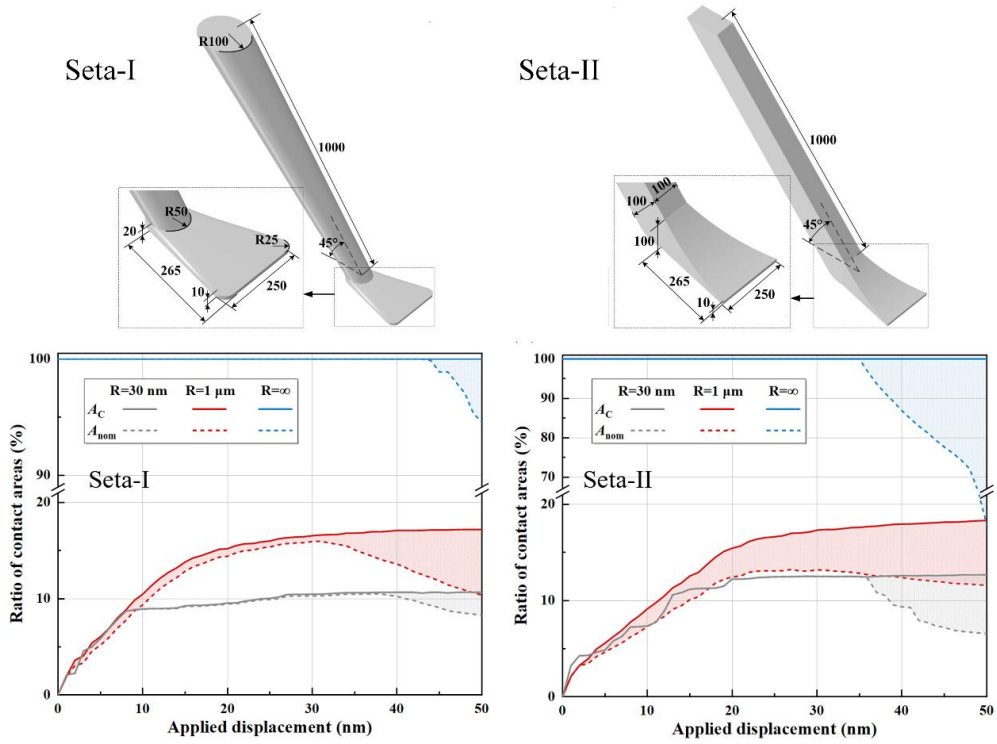



**Figure 12 Two synthetic adhesive prototypes and their corresponding real contact areas on rough surfaces.**
Reproduced with permission. Cheng Q, Jiang Z, Borodich FM, Gorb SN, Jin X. Interaction of a non-axisymmetric artificial single spatula with rough surfaces. *Interface Focus*. 2024;14(3):20230081. Copyright 2024, The Royal Society.

**Biomimetic adhesives based on polygon arrays**

The polygonal microcolumn geometry on tree frog toes enables their thriving in humid environments. In addition to vdW forces directly generated by contact between these microcolumns and solid surfaces, wet adhesive forces are also involved. This is because liquid bridges form between the polygonal microcolumns on tree frog footpads and the contact surface, generating capillary forces as shown in Eq. (7). Various polygonal microcolumns are observed on tree frog toe pads, with hexagonal microcolumns being predominant. Chen et al. systematically compared frictional forces across seven different surface patterns and concluded that hexagonal microcolumns exhibit superior adhesive performance. Hexagonal microcolumns on tree frog footpads exist in various types, such as slender and regular hexagonal microcolumns, which may differ in size and arrangement [99]. Based on the classification of hexagonal patterns, Iturri et al. compared the frictional forces of slender and regular hexagonal microcolumns, finding that under humid conditions, slender hexagonal structures generate greater friction than regular ones [100]. This is attributed to their reduced bending stiffness and increased edge density along the direction of movement. Additionally, Iturri et al. investigated the effect of microcolumn height, revealing that friction differences between columns with a height of 5–10 are nearly negligible [100]. However, when column height increases to 20, excessive deformation of the columns leads to a significant reduction in friction under humid conditions. This deformation causes column aggregation, thereby reducing the contact area. Beyond the effects of shape and height on adhesive force, Xie et al. extensively studied the influence of additional parameters on the adhesive performance of hexagonal structures, finding that interactions between height, width, and length ratios also significantly impact the performance of hexagonal array adhesives [101].

Interlaced microscale groove structures surrounding the polygonal microcolumns of tree frogs also play a critical role in their adhesive performance. The groove structures of tree frog footpads form an organic functional collaboration: when toe pads need to bend over distances larger than the block size, the grooves naturally increase contact area and adhesive force with the substrate by reducing their own elasticity. Liquid stored in the grooves acts as a natural reservoir, directly assisting tree frogs in rapidly adhering to rough substrate surfaces— a characteristic crucial for achieving firm and rapid attachment. Furthermore, in liquid environments, the grooves promote drainage of liquid between the toe pads and the substrate to form capillary bridges, thereby triggering capillary action to enhance adhesive ability. During heavy rain, when tree frogs retract their feet rapidly, channels between the outer boundary cells of the toe pads may close, producing an effective “suction-like” adhesive effect on submerged surfaces. Thus, such groove structures are highly necessary. Regarding the influence of these groove structures on adhesion, Gupta, Fréchette et al. directly measured normal hydrodynamic interactions of fluids between structured and smooth surfaces through experiments using biomimetic structured surfaces, concluding that the groove structures of tree frog footpads can indeed reduce hydrodynamic repulsion through drainage, thereby promoting adhesion [102].

In the process of transforming biological prototypes into engineering materials, roll-to-roll nanoimprinting technology provides an effective approach for the large-scale preparation of biomimetic adhesives based on the polygonal arrays of tree frog toes. Through roll-to-roll nanoimprinting, the hexagonal microcolumn structures on tree frog toes and the microscale groove structures around them can be accurately replicated on the surface of large-area materials. When replicating hexagonal microcolumns, this technology can precisely control the size, shape, and arrangement of the microcolumns, ensuring that each microcolumn maintains a consistent structure during large-scale production, thereby guaranteeing the stable adhesion performance of the adhesive. For microscale groove structures, roll-to-roll nanoimprinting technology can also achieve high-precision replication, making the depth, width, and connectivity of the grooves meet the design requirements. This helps to better exert the functions of drainage and enhancing capillary action in humid environments, thereby improving the overall performance of the biomimetic adhesive.

Through the collaborative design of these micro-nano scale surface

structures on tree frog footpads, tree frogs achieve a balance between strong adhesion and flexible detachment in humid and rough environments. This provides a biological prototype for geometric optimization in biomimetic adhesive design.

**Biomimetic adhesives based on sucker arrays**

In nature, numerous organisms with sucker structures can achieve high-strength adhesion underwater, relying on these structures to assist in adhesion. For instance, the arms of octopuses are covered with dense sucker arrays, and the protruding surface of each sucker is further covered with a layer of dense hair-like setal arrays. This structure effectively enhances the sealing between the suckers and the substrate, thereby ensuring the generation of reliable suction [3, 43, 103]. The remora has a circular sucker on the top of its head, with parallel spiked plate structures distributed around the disc, which increases friction between the disc and the substrate. This enables the remora to exhibit underwater "hitchhiking" behavior [104, 105]. Aquatic organisms such as blennies and sucker-mouthed catfish also possess sucker structures. Despite morphological differences in their sucker structures, all these organisms utilize suckers for negative pressure adsorption, and the sucker surfaces feature micro or nano-scale structures to enhance sealing between the attachment structure and the substrate [106].

Taking the octopus sucker array system as an example, the octopus is a typical marine organism model that uses suckers to achieve reliable underwater adhesion. The key to its underwater adhesive ability lies in negative pressure suction, which is directly determined by the pressure difference and effective contact area. Thus, ensuring good sealing and adaptability to the contact interface is critical for maximizing the pressure difference and effective contact area, thereby achieving excellent adhesive force [106]. Many researchers have found that artificial suckers mimicking the surface of octopus sucker arrays exhibit enhanced adhesion. Baik et al. successfully developed biomimetic sucker array adhesives with adhesion performance comparable to that of octopuses by imitating the array structure of octopus sucker surfaces [107]. These suckers are equipped with internal curved cavities to reduce edge modulus, promote conformal contact with the substrate, and ensure effective sealing. They also studied the influence of the radius of curvature on these suckers, finding that a curvature of 0.93 produces a larger effective contact area and optimal switchable adhesive force. Additionally, Baik et al. integrated micro-domes with protrusions on the top of the suckers into the sucker array structure, utilizing cohesive forces between liquid molecules to generate an additional capillary-assisted suction effect, thereby forming a structure with stronger wet adhesive force [45].

The excellent adhesive performance of biological sucker array structures stems not only from unique morphological designs but also from microscale physical mechanisms. Spolenak et al. studied the influence of contact shape on adhesion and concluded that annular contact geometry provides better contact connection and thus more excellent adhesive force [78]. The contact shape of these biological sucker structures is precisely circular, a characteristic that ensures stable adhesion in complex fluid environments. As mentioned earlier, the sucker array adhesives developed by Baik et al. require effective sealing, as larger suckers are prone to pressure leakage due to imperfect conformal contact, leading to a significant decrease in suction force [45, 107]. Smith et al. addressed this issue as early as 1996, finding that smaller suckers can generate higher pressure differences than larger ones [108]. This is because smaller cavities experience lower circumferential stress, enabling them to withstand greater pressure differences. Due to the many advantages of sucker arrays, they have been applied in various industrial scenarios, such as the medical field, for biological signal detection and postoperative wound healing, among others.

The development of roll-to-roll nanoimprinting and hybrid manufacturing technologies has brought a breakthrough in the large-scale production of octopus-inspired suction cup array biomimetic adhesives. Using roll-to-roll nanoimprinting technology, suction cup arrays with precise micro/nano structures can be manufactured on flexible materials on a large scale. By designing special templates, the macroscopic cavities and microscopic surface textures of octopus suction cups can be replicated. For example, during the manufacturing process, the curvature and depth of the suction cup cavities, as well as the shape and distribution of surface micro/nano structures, can be precisely controlled. This enables the biomimetic suction cups to better adapt to different surfaces while ensuring sealing performance. In addition, combining hybrid manufacturing technologies such as 3D printing can further optimize the structure of the suction cups. For instance, adding special sealing materials to the edges of the suction cups or integrating functional components like sensors inside them can enhance the performance and expand the application range of the biomimetic suction cups, promoting their large-scale application in fields such as medical treatment and underwater operations.

**Biomimetic adhesives based on hybrid structures**

In previous chapters, gecko-inspired dry mushroom array adhesives, tree frog-inspired polygonal array wet adhesives, and octopus-inspired sucker array adhesives have been discussed. These adhesives exhibit high-strength adhesion in specific scenarios but also have obvious limitations. For example, although the gecko's micro-nano mushroom array structure demonstrates high adhesion under dry conditions, can be reused, and achieves high-strength adhesion on smooth surfaces, it has clear drawbacks: it functions only under dry conditions, with adhesion potentially failing in humid environments. Similarly, tree frog polygonal column array adhesives rely heavily on capillary action from liquid bridges between the surface and the substrate, leading to weakened adhesion in dry environments. Octopus-type sucker array adhesives suffer from the limitation that sucker sealing performance is significantly affected by surface roughness, making it difficult to form complete negative pressure on complex curved surfaces. However, integrating the advantages of two or more single structures can compensate for the defects of a single mechanism, achieving a "synergistic effect" greater than the sum of individual parts.

To address the deficiency of gecko footpad mushroom structures in wet environments, Lee et al. coated a thin layer of mussel-inspired polymer film on the surface of a series of gecko-inspired nanoscale microcolumns, endowing them with strong and reversible wet/dry adhesion [109]. Experimental validation shows that compared with traditional gecko-inspired adhesives, this gecko-mussel hybrid adhesive not only improves dry adhesion but also significantly enhances wet adhesion, with the adhesion of each pillar increasing from 5.9 nN to 86.3 nN under wet conditions, confirming the effectiveness of this hybrid adhesive structure. Similarly, Dayan et al. innovatively integrated the dome-shaped protrusion structure of octopus suckers onto the top of gecko mushroom-type micro-nano columns, developing a gecko-octopus hybrid bionic adhesive [110]. This adhesive incorporates octopus-like patterns on the surface of ultrafine fiber tips, enhancing wet adhesion under preload by generating cohesion between liquid molecules, thus achieving wet adhesion performance. Both cases above are based on gecko mushroom arrays, with wet adhesion capability realized by integrating other wet adhesion components. Kim et al. adopted octopus-like convex cups on the top surface of tree frog hexagonal columns, enabling the adhesive to maintain high-strength adhesion under both wet and dry conditions while retaining omnidirectional tear resistance [111]. This design utilizes the groove structures around the hexagonal microcolumns on the tree frog footpad surface, which act as "drainage channels" to quickly expel water or air between the footpad and the substrate, bringing the foot closer to the surface. Meanwhile, these grooves increase surface roughness, overcoming the poor surface adaptability of sucker structures.

Due to the complementary nature of these hybrid-structured bionic adhesives, which offset the shortcomings of individual structures while leveraging their advantages, they hold significant application value in the biomedical field, particularly in biomedical patches [109–111]. Recent studies by LingHu et al. have shown that the aphid-inspired magnetically driven hybrid structure adhesive achieves

rapid switching of adhesion strength with a switching ratio of up to 64:1 by regulating the contact area through magnetically controlled film deformation. It can also work stably in a vacuum environment, providing a new solution for the precise transfer printing of biomedical patches such as device positioning in minimally invasive surgeries [112]. Its magnetic response mechanism can synergize with the van der Waals forces of gecko setae or the negative pressure effect of octopus suckers, further enhancing operational flexibility in complex physiological environments.

## Applications of biomimetic adhesives in the medicine

In summary, incorporating bioinspired structural principles into surface design enables bioinspired adhesives to exhibit outstanding performance in environmental adaptability, terrain conformity, and controllable adhesion. In recent years, these adhesives have attracted significant attention in the field of biomedical engineering, particularly in applications such as medical monitoring, soft tissue gripping, and drug delivery, as shown in Figure 13 [8, 111, 113–116].

**Medical monitoring**

Bionic adhesives exhibit enormous application potential, particularly in the biomedical field, due to their versatility and strong environmental adaptability. The first application area is medical physiological signal detection. Recent studies indicate that stable adhesion and long-term wearing comfort constitute the primary challenge limiting the application of wearable devices in real-time health monitoring. The surface of human skin and tissues is microscopically complex; while some traditional adhesives perform well on flat surfaces, their interfacial adhesion on human skin may be significantly reduced, especially under conditions such as exercise and sweating, where many traditional adhesives fall short. Bionic adhesives, based on the adhesive microstructures of natural animals, have thus become the optimal material choice to address these issues. In recent years, extensive research by domestic and international teams has led to the widespread development of wearable bioelectronic devices for physiological signal monitoring [8, 9, 113, 117–123], as shown in Figure 14. To clearly show the different application scenarios, inspiration sources, design features, references, and advantages of bionic adhesives in medical monitoring, Table 1 is presented. Wearable devices combining natural microstructured adhesives and physiological signal sensors avoid the aforementioned problems. For example, Wang et al. developed a novel brain-computer interface (BMI) using mussel-inspired hydrogel [121]. Since the subdural electrodes of the BMI must be implanted on the surface of the cerebral cortex during surgery, the patch made from this bionic hydrogel ensures non-destructive and stable fixation of the BMI in the dynamic brain environment. This is because it prevents micromotion between the electronic device and tissues, which would otherwise inevitably cause damage or inflammation. The bioadhesives of the hydrogel ensures tight bonding with metal microcircuits and seamless contact with brain tissue. Another example is the dry adhesive developed by Drotlef et al., which integrates the mushroom-shaped columnar structure of gecko setal arrays, as shown in Figure 14c [9]. The skin adhesive film made from this dry adhesive is used in wearable devices, integrated with strain sensors for respiratory and heart rate monitoring, achieving firm adhesion on the skin and high signal enhancement. Similarly, Kwak et al. developed a novel medical skin patch inspired by geckos. In their study, while ensuring adhesive strength, they identified optimal conditions for dry adhesive skin patches through combinations of various microcolumn structural and material parameters, as shown in Figure 14a [119]. There are also octopus-inspired dry adhesive physiological signal sensors for continuous vital sign monitoring, as shown in Figure 14b [8]. A common feature of these bionic structured dry adhesives is that they enhance adhesion and comfort while minimizing tissue damage and skin inflammation, exhibiting good biocompatibility.

In addition to the applications of dry bionic adhesives in medical wearable devices, wet adhesives for scenarios such as patient sweating in physiological signal monitoring sensors have also attracted significant attention [111, 113, 122, 123], as shown in Figure 14. Most wet adhesives are inspired by the hexagonal cell patterns on tree frog footpads and the sucker arrays of octopuses. These organisms are inherently aquatic species, and their microscopic array structures contribute to their adaptation to humid environments. Adhesives developed under such biological inspirations also demonstrate excellent performance in medical physiological signal monitoring. For example, inspired by the excellent wet adhesion of tree frog toe pads, Zhang et al. proposed a wet adhesive surface that utilizes the self-splitting and self-suction effects of tree frog footpad surfaces to enhance the formation of liquid bridges, thereby improving wet adhesion, as shown in Figure 14d [113]. This has been applied in wearable flexible electronics, with results showing that electronic sensors integrated with tree frog footpad surface features can still distinguish pulse signals when the skin is sweaty. Another representative example of wet adhesion is inspired by octopuses. Lee et al. proposed a bilayer adhesive patch with enhanced dynamic adhesion performance, inspired by octopus sucker arrays, using an octopus-inspired architecture (d-OIA) coated with a soft elastomer [123]. By mimicking the actual tissue structure of octopus suckers, which are composed of two layers with different moduli, this adhesive patch can maintain a vacuum state in the chamber. This enables stable monitoring of electrocardiogram (ECG) and electromyogram (EMG) signals even under conditions of rough skin, movement-induced bending and stretching, or sweating. It also maintains high compatibility with biological skin and tissues. However, adhesives combining only the hexagonal structure of tree frog footpads or only the octopus sucker array structure have certain limitations. The hexagonal structure of tree frogs performs well in drainage efficiency and peel resistance but has limited vertical adhesive force. Especially under strong water flow or high humidity, the patch may fall off due to insufficient suction. Although the octopus sucker structure has excellent vertical adhesion, the lack of a systematic drainage architecture leads to significantly reduced adsorption efficiency due to interfacial liquid accumulation. To overcome these defects, Kim et al. combined the two structures to develop a tree frog-octopus hybrid model, embedding octopus sucker arrays in hexagonal cells while retaining the channel structure of tree frog hexagonal structures, as shown in Figure 14f [111]. The flexible physiological signal sensor made from this structure avoids falling off caused by water accumulation, ensures strong adhesive capability of the sensor patch, and maintains stable signal monitoring. Similarly, Lan et al. proposed a structured electrode inspired by tree frog footpads, as shown in Figure 14e [122], which features high adhesion and permeability and can be used for long-term physiological signal monitoring. Their work provides new design ideas for physiological signal sensors based on bionic materials.

**Table 1 Medical monitoring applications**

| Scenarios | Inspiration | Design | References | Advantages |
|---|---|---|---|---|
| Wearable devices | Gecko octopus | Mushroom microcolumns | [8, 9, 117–119] | Strong adhesion, Biocompatible, Humid-resistant |
| Wet monitoring | Tree frog octopus | Hexagonal columns | [111, 113, 122, 123] | Drainage-efficient, Stable on rough skin |
| BMI | Mussel | Hydrogel patches | [121] | Seamless tissue fit micromotion inhibition |

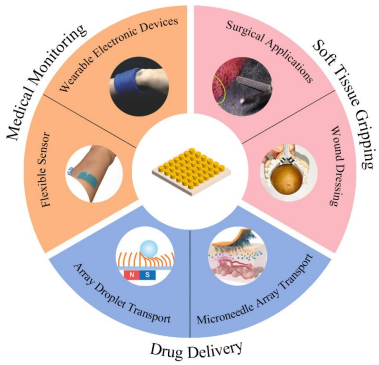



**Figure 13 Various biomedical applications of bioinspired microstructure.**
Reproduced with permission. Choi MK, Park OK, Choi C, et al. Cephalopod-Inspired Miniaturized Suction Cups for Smart Medical Skin. *Adv Healthc Mater*. 2016;5(1):80–87. Copyright 2016, WILEY. Kim DW, Baik S, Min H, et al. Highly Permeable Skin Patch with Conductive Hierarchical Architectures Inspired by Amphibians and Octopi for Omnidirectionally Enhanced Wet Adhesion. *Adv Funct Mater*. 2019;29(13):1807614. Copyright 2019, WILEY. Zhang L, Chen H, Guo Y, et al. Micro–Nano Hierarchical Structure Enhanced Strong Wet Friction Surface Inspired by Tree Frogs. *Adv Sci*. 2020;7(20):2001125. Copyright 2020, WILEY. Hoang TT, Quek JJS, Thai MT, Phan PT, Lovell NH, Do TN. Soft robotic fabric gripper with gecko adhesion and variable stiffness. *Sens Actuators A*. 2021;323:112673. Copyright 2021, Elsevier. Jing X, Chen H, Zhang L, et al. Accurate Magneto-Driven Multi-Dimensional Droplet Manipulation. *Adv Funct Mater*. 2022;33(9):2210883. Copyright 2022, WILEY. Zhao L, Zhang C, Abu-Ershaid JM, et al. Smart Responsive Microarray Patches for Transdermal Drug Delivery and Biological Monitoring. *Adv Healthc Mater*. 2021;10(20):2100996. Copyright 2021, WILEY.

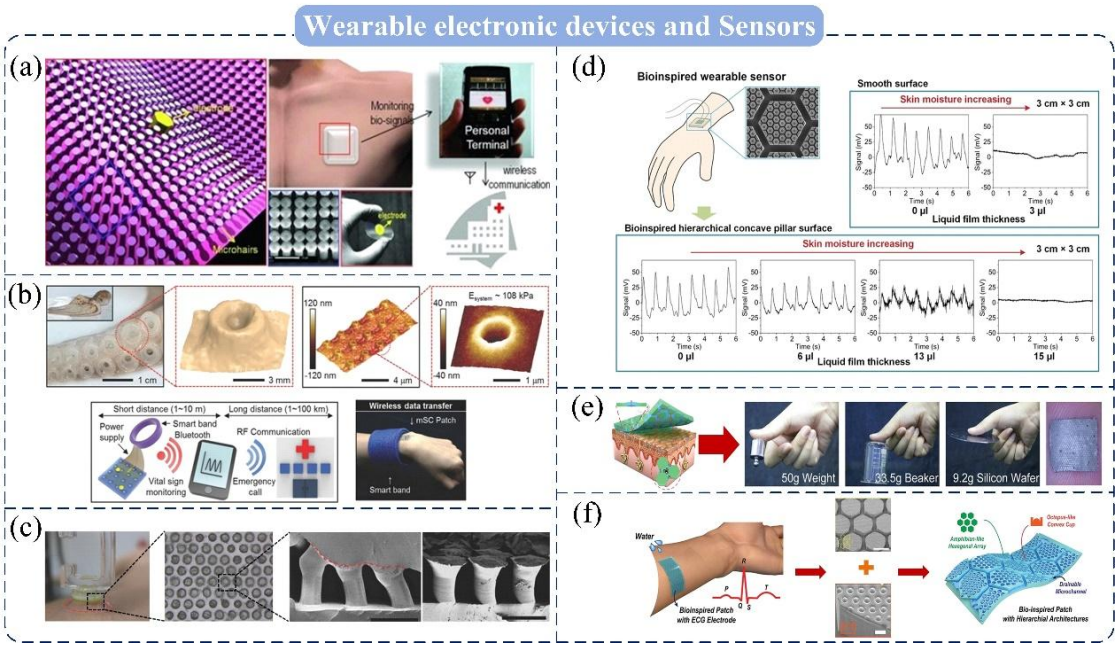



**Figure 14 Wearable electronic devices and sensors enabled by bioinspired adhesives.**
(a) Conceptual diagram of a real-time diagnostic system using dry adhesives as biomedical bandages. Reproduced with permission. Kwak MK, Jeong H, Suh KY. Rational Design and Enhanced Biocompatibility of a Dry Adhesive Medical Skin Patch. *Adv Mater*. 2011;23(34):3949–3953. Copyright 2011, WILEY. (b) Schematic diagram of a wearable electronic monitoring device adopting bionic multifunctional micro-suction cup dry adhesives. Reproduced with permission. Choi MK, Park OK, Choi C, et al. Cephalopod-Inspired Miniaturized Suction Cups for Smart Medical Skin. *Adv Healthc Mater*. 2016;5(1):80–87. Copyright 2016, WILEY. (c) Schematic diagram of the skin adhesive membrane on the forearm during the retraction phase of the adhesion experiment, along with its cross-sectional SEM image. Reproduced with permission. Drotlef D, Amjadi M, Yunusa M, Sitti M. Bioinspired Composite Microfibers for Skin Adhesion and Signal Amplification of Wearable Sensors. *Adv Mater*. 2017;29(28):1701353. Copyright 2017, WILEY. (d) On smooth surfaces, moist skin leads to weak adhesion and indistinct pulse signals; whereas on bioinspired concave pillar surfaces, pulse signals remain distinguishable even with a liquid film. Reproduced with permission. Zhang L, Chen H, Guo Y, et al. Micro–Nano Hierarchical Structure Enhanced Strong Wet Friction Surface Inspired by Tree Frogs. *Adv Sci*. 2020;7(20):2001125. Copyright 2020, WILEY. (e) Web-like electrodes exhibit high adhesion to heavy objects and conform well to the thumb tip. Reproduced with permission. Lan T, Tian H, Chen X, et al. Treefrog-Inspired Flexible Electrode with High Permeability, Stable Adhesion, and Robust Durability. *Adv Mater*. 2024;36(31):2404761. Copyright 2024, WILEY. (f) Schematic diagram of an adhesive sensor integrating the structures of amphibian footpads and octopus suckers for biological signal monitoring. Reproduced with permission. Kim DW, Baik S, Min H, et al. Highly Permeable Skin Patch with Conductive Hierarchical Architectures Inspired by Amphibians and Octopi for Omnidirectionally Enhanced Wet Adhesion. *Adv Funct Mater*. 2019;29(13):1807614. Copyright 2019, WILEY.

Bionic adhesives exhibit significant application potential in the biomedical field. By mimicking the adhesive structures of animals such as tree frogs and octopuses, they overcome the adhesion limitations of traditional adhesives on human skin, particularly in wet environments. Dry adhesives achieve strong adhesion and biocompatibility through geometric interlocking or molecular interactions, while wet adhesives integrate the drainage mechanism of tree frogs and the suction mechanism of octopuses to enhance stability under wet conditions. For instance, hybrid structure patches combine the advantages of both types, preventing liquid accumulation and enhancing adhesion. This enables stable physiological signal monitoring in dynamic wet environments, providing innovative solutions for wearable medical devices.

Although current biomimetic adhesives show potential in medical monitoring, they still face significant challenges. When in long-term contact with the skin, synthetic materials may cause local skin discomfort, and some users may experience mild redness or itching. Dynamic physiological environments such as sweating or skin stretching can lead to premature detachment of dry adhesives, while wet adhesives may struggle to maintain stable signal collection due to the breakage of liquid bridges. For implantable monitoring devices, fibrous tissue encapsulation may occur around the adhesive interface, which could affect the signal transmission efficiency over time. Addressing these issues requires optimizing the biocompatibility of materials, developing milder surface treatment methods, and improving the adaptability of adhesives to dynamic skin changes through structural design.

**Soft tissue gripping**

In the field of medical surgery and trauma repair, bionic adhesives are gradually transforming traditional technical paradigms. These materials achieve precise and non-invasive fixation and repair of biological tissues by mimicking natural adhesion mechanisms, such as geckos' microstructured dry adhesion, tree frogs' and mussels' wet adhesion, and octopuses' suction-cup-based controllable adhesion. Their core advantages lie in the integration of high biocompatibility, tunable adhesion strength, and dynamic response capability, which perfectly adapt to the complex physiological environment of soft tissues. Compared with invasive methods like suturing or stapling, bionic adhesives significantly reduce the risk of tissue damage and infection, simplify the operation process, and provide a new pathway for minimally invasive surgery and efficient wound repair. To systematically summarize the application scenarios, inspiration sources, design features, references, and advantages of bionic adhesives in soft tissue gripping, Table 2 is presented.

Flexible grasping devices utilize bionic adhesion mechanisms to enable safe manipulation of human tissues. Bionic adhesives inspired by different animals can significantly reduce surgical risks when applied to surgical grasping instruments. For example, Mahdavi et al. developed a biodegradable gecko-inspired bioadhesive that achieves reversible adhesion without chemical adhesives by mimicking gecko footpads. It can be used as a surface coating for surgical instruments, and experimental verification has shown that it elicits minimal human tissue response [10]. Hoang proposed a soft robotic gripper with variable stiffness based on geckos' setal structure, as shown in Figure 15c [114], which maintains effective grasping capability. This novel design provides important references for surgical tissue grasping devices. Song et al. designed an adhesive with spherical chambers and mushroom-shaped tips inspired by diving beetles, successfully applying this diving beetle-style adhesive to the top surface of surgical graspers, as shown in Figure 15b [11]. By using bio-inspired structures as highly conformal and wet-resistant adhesive elements, they minimized damage to the engaged liver surface. In addition to dry adhesion applications, wet adhesion based on octopuses' suction cup array structures adapts to wet and slippery surfaces through vacuum adsorption. For instance, Wu et al. developed a strong, switchable, and biocompatible adhesive patch by imitating the edges of octopus suction cups, which was successfully applied to laparoscopes [124]. Results showed that such laparoscopes with bionic patches reduced mechanical damage to tissues during procedures like liver retraction. Similarly, tree frog-inspired wet friction surfaces extrude interfacial liquids through micro-nano hierarchical structures, providing strong friction in wet environments. Wet adhesives inspired by tree frog structures, when applied to surgical forceps, can significantly reduce the clamping force required, thereby minimizing mechanical damage to tissues [99], as shown in Figure 15a [113]. Furthermore, there are applications of adhesives combining two structures. For example, Ahmad et al. ingeniously designed an adhesive integrating tree frogs' hexagonal structures and octopuses' suction cup structures [125]. Combining the characteristics of these two animals, the adhesive patch exhibits excellent multi-environmental adaptability, adhesion strength, and long-term stability, showing great application value in non-damaging surgical instruments. In minimally invasive surgery, these instruments address the limitations of traditional rigid tools. Electrostatic/gecko-inspired soft grippers enhance grasping force through switchable adhesion, making them suitable for manipulating fragile tissues such as internal organs or tumors, and their integrated adhesive layers maintain performance on rough surfaces [126]. Theoretical models indicate that combining fiber-reinforced actuators with bionic adhesives can optimize the grasping angle and blocking force for cylindrical organs [127].

In trauma repair, aquatic animals' suction cup array structures—especially those of octopuses—hold enormous application value, with hydrogel-based devices made from these structures playing a core role. For example, Lee et al. designed a small hydrogel adhesive robot that achieves controllable tissue adhesion and gentle separation through an octopus-inspired adhesive for minimally invasive interventional therapies such as targeted drug delivery [128]. The hydrogel can achieve controllable tissue adhesion under an externally applied magnetic field to facilitate trauma repair, while its biocompatibility reduces inflammatory responses. Huang et al. designed a multifunctional wound patch using customizable micro-suction cup patterns, as shown in Figure 15d [12]. In the field of tissue repair, degradable biomedical elastomers (DBE) exhibit significant advantages as tissue adhesives, with their core strength lying in the precise matching between their controllable degradation properties and the tissue repair cycle. For example, polyglycolic acid (PGA), a typical medical elastomer, degrades in vivo through hydrolysis: its mechanical properties show a noticeable decline within 1–2 months, and its mass gradually decreases over 6–12 months, eventually degrading into glycine, which can be excreted through urine or metabolized into carbon dioxide and water. This degradation cycle is highly compatible with the healing process of skin trauma, including the inflammatory phase 1–7 days, proliferative phase 3–21 days, and remodeling phase over 21 days. It can provide stable adhesive support while avoiding foreign body reactions caused by long-term residues [129]. The elastic material Eco-flex is cast using a mold method to produce customizable suction cup arrays, and a gelatin-based photosensitive hydrogel customized for the wound shape is polymerized as needed. This material can reversibly adhere to wounds, induce cell adhesion, deliver drugs, and ultimately promote wound healing. Zhang et al. developed a hydrogel patch integrating adhesion, antibacterial, and drug delivery functions [130]. The elastic substrate of its suction cup array is mainly made from a mixture of polydopamine and gelatin. Each suction cup in the array has a diameter of several hundred micrometers and internal protrusions. Under the synergistic effect of the suction cups and catecholamines, the array can generate a peeling adhesion force exceeding 1 N/cm$^2$ at dry-wet interfaces and can function repeatedly through 10 adhesion-peeling cycles. This patch shows great application potential in wound repair [131]. Breaking free from the constraints of traditional medical patches for trauma repair, Lee et al. proposed a small soft robot with an octopus-inspired biocompatible hydrogel adhesive (OHA) featuring strong wet adhesion, which can be used for in vivo tissue trauma repair, as shown in Figure 15e [128]. Verification has confirmed that when the small soft OHA robot operates in vivo, its strong adhesion to biological tissues and controllable separation enable effective achievement of biomedical

functions.

In the field of medical surgery and trauma repair, bionic adhesives enable precise and non-invasive fixation of biological tissues by mimicking mechanisms such as geckos' microstructured dry adhesion, mussels' wet adhesion, and octopuses' suction-cup-based controllable adhesion. Their core advantages include high biocompatibility, tunable adhesion strength, and dynamic response capability, which significantly reduce the risks of tissue damage and infection while simplifying operational processes. In flexible grasping instruments, adhesives inspired by geckos and octopuses enhance the safety of manipulating fragile tissues. In trauma repair, hydrogel-based devices integrated with drug delivery functions effectively promote wound healing. These innovative technologies offer new paradigms for minimally invasive surgery and efficient tissue repair.

In surgical procedures and trauma repair, biomimetic adhesives need to balance adhesive strength and biocompatibility, and this process is confronted with multiple challenges. Moist tissue surfaces covered with mucus can weaken the adhesive effect of dry adhesives, resulting in insufficient grasping stability. Octopus-like suction cups are prone to poor sealing on irregular tissue surfaces; if preloading force is increased to enhance sealing, it may cause damage to fragile tissues. Degradable adhesives may degrade too quickly in high-humidity environments, losing their adhesive ability before the tissues complete healing. In the future, it will be necessary to enhance the adhesive force in wet environments through hierarchical microstructure design and develop a controllable degradation mechanism that matches the tissue repair cycle.

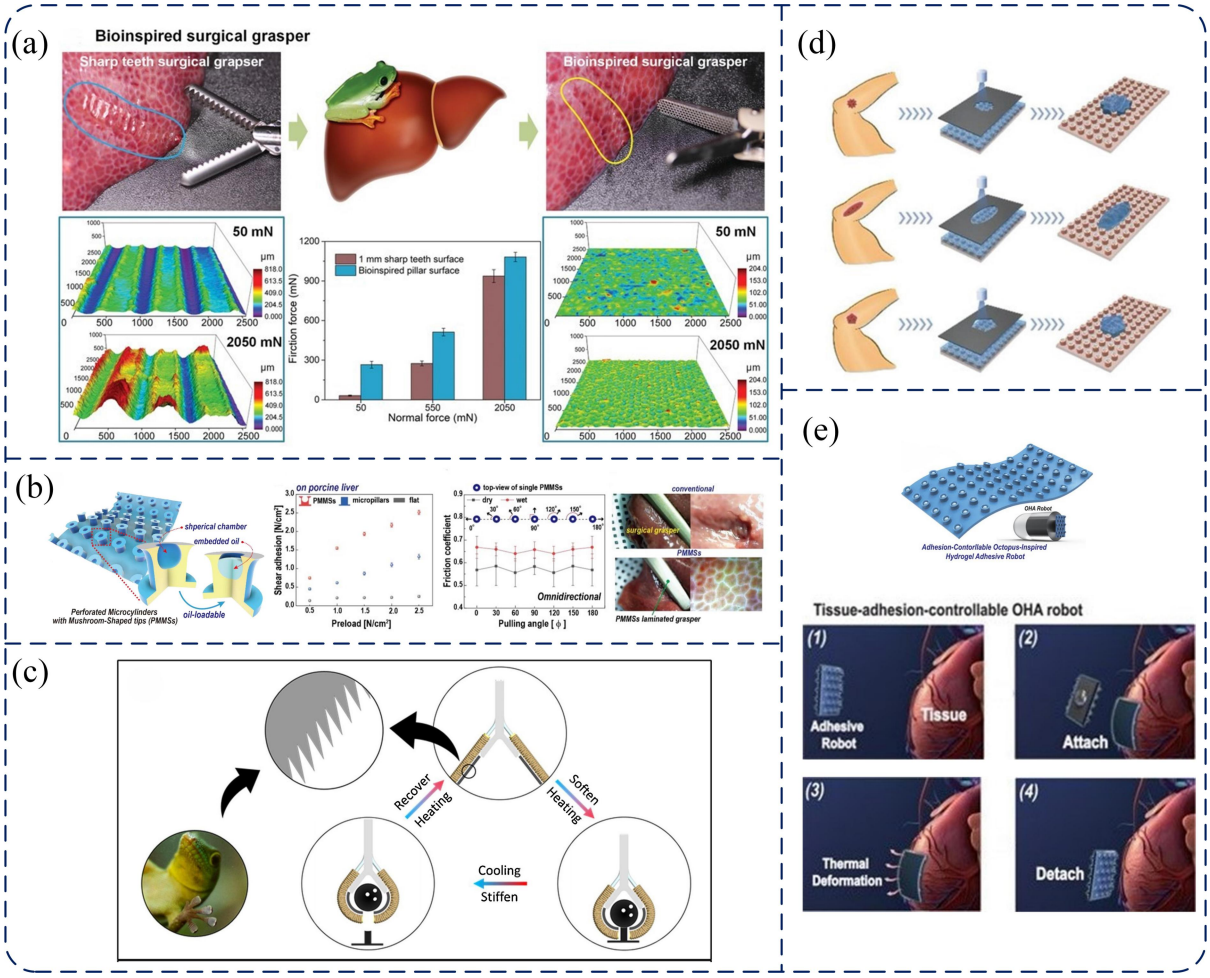



**Figure 15 Bioinspired adhesive solutions for surgical and robotic applications.**

(a) The tissue deformation and friction performance have been characterized on 1 mm sharp teeth surface and bioinspired hierarchical concave pillar surface. Based on the safety grasping threshold of pig liver, normal load of 50, 550, and 2050 mN were applied during friction measurement. Bioinspired surface shows much lower tissue deformation and stronger friction than modern sharp teeth surface. Reproduced with permission. Zhang L, Chen H, Guo Y, et al. Micro–Nano Hierarchical Structure Enhanced Strong Wet Friction Surface Inspired by Tree Frogs. *Adv Sci*. 2020;7(20):2001125. Copyright 2020, WILEY. (b) The characteristics of mushroom-shaped tips for grasping perforated microcylinders on mucus-coated organs and the comparison of shear adhesion strength of different control samples on smooth porcine liver tissue. Reproduced with permission. Song JH, Baik S, Kim DW, Yang TH, Pang C. Wet soft bio-adhesion of insect-inspired polymeric oil-loadable perforated microcylinders. *Chem Eng J*. 2021;423:130194. Copyright 2021, Elsevier. (c) Illustration of a soft fabric gripper with enhanced performance via incorporation of a gecko adhesive and a thermo-responsive VSF. Reproduced with permission. Hoang TT, Quek JJS, Thai MT, Phan PT, Lovell NH, Do TN. Soft robotic fabric gripper with gecko adhesion and variable stiffness. *Sens Actuators A*. 2021;323:112673. Copyright 2021, Elsevier. (d) Schematic illustration of the bioinspired skin-adhesive patch with tailorable wound dressing. Reproduced with permission. Huang R, Zhang X, Li W, Shang L, Wang H, Zhao Y. Suction Cups-Inspired Adhesive Patch with Tailorable Patterns for Versatile Wound Healing. *Adv Sci*. 2021;8(17):2100201. Copyright 2021, WILEY. (e) A small octopus-inspired hydrogel adhesive (OHA) robot with controllable tissue adhesion and biocompatibility attaches to and detaches from tissue surfaces with controllable wet adhesion for future minimally invasive biomedical functions. Reproduced with permission. Lee Y, Chun S, Son D, Hu X, Schneider M, Sitti M. A Tissue Adhesion-Controllable and Biocompatible Small-Scale Hydrogel Adhesive Robot. *Adv Mater*. 2022;34(13):2109325. Copyright 2022, WILEY.

Table 2 Soft tissue gripping applications

| Scenarios | Inspiration | Design | References | Advantages |
|---|---|---|---|---|
| Surgical tools | Gecko diving beetle | Mushroom columns | [10, 11, 113] | Low-damage strong wet friction |
| Minimally invasive | Octopus tree frog | Sucker edges | [124, 125] | Wet-adaptable controllable adhesion |
| Trauma repair | Octopus | Hydrogel suckers | [12, 128] | Biocompatible reversible adhesion |

**Drug delivery**

Bionic adhesives exhibit revolutionary potential in drug transport by leveraging their bio-inspired adhesive mechanisms to overcome key challenges in drug delivery, such as unstable interfacial contact, premature detachment, and inefficient targeting. Their core advantage lies in integrating specific adhesion principles derived from natural organisms with intelligent drug release functions, thereby enhancing transdermal efficiency, ensuring sustained contact, and improving therapeutic precision, which significantly enhance transdermal drug delivery efficiency, wound healing effects, and patient comfort. Wet adhesives, in particular, hold enormous application value in drug transport. To systematically summarize the application scenarios, inspiration sources, design features, references, and advantages of bionic adhesives in drug delivery, Table 3 is presented. For example, Inspired by the suction cup structures of cephalopods, Choi et al. developed a micro-suction cup (mSCs)-based intelligent medical skin system [8]. This design utilizes both van der Waals forces from ultra-soft materials and negative pressure-induced suction to achieve seamless adhesion to the skin. This dual adhesion mechanism prevents detachment caused by skin movement or sweating, ensuring continuous drug delivery without irritation. Its innovation lies in embedding stretchable electronics for vital sign monitoring while retaining adhesion during multiple drug reloads, highlighting how adhesion stability directly enables long-term transdermal therapy [8]. Inspired by octopus suction cups, Huang et al. proposed a customizable patterned adhesive patch [12], which employs template replication to mimic the sucker's sealing and pressure-regulating structures. The patch's selective adhesion achieved through precisely controlled suction cup arrays ensures firm attachment to irregular skin surfaces allowing personalized drug release while avoiding accidental displacement. This demonstrates how bio-inspired adhesion enables both targeting and retention in dynamic physiological environments. The setal microcolumn array structure of beetle legs has also inspired advances in drug transport [132, 133]. Tsai et al. inspired by the microcolumn structure of beetle feet, designed a self-adhesive transdermal drug delivery patch [132]. This drug-loaded transdermal delivery system microcolumn patch is fabricated by combining bionic microcolumn arrays with polydimethylsiloxane elastomers, enabling reusability and controllable drug release. The setal microcolumn array structure of beetle legs which relies on van der Waals forces and capillary action for adhesion has also inspired advances in drug transport. Tsai et al. designed a self-adhesive transdermal patch by combining such bionic microcolumn arrays with polydimethylsiloxane elastomers, the microcolumns' high surface area enhances interfacial contact generating sufficient adhesion to resist bodily fluids while their reversible adhesion allows repeated application [132]. Similarly, Baik et al. mimicked the plunger mechanism of diving beetles to develop an integrated micro-plunger device [133]. This device rapidly captures biological fluids through reversible negative pressure, adheres to the skin surface, and integrates machine learning for intelligent skin care. Its micro-plunger structure can complete fluid sampling within seconds while releasing antibacterial or anti-inflammatory drugs, making it particularly effective in delivering drugs for treating common acne.

In the field of drug delivery, beyond traditional systems based on physical structure bionics and wet adhesion mechanisms, dynamic transport technologies regulated by magnetic fields have emerged as a research focus in recent years [134–138], as shown in Figure 16. The directional transport of droplets by magnetically controlled bionic arrays offers multiple technical advantages, including excellent biocompatibility, remote non-contact control, and instantaneous response [139]. Building on these magnetically controlled simulation arrays, Ben et al. designed and constructed a biomimetic hydrophobic magnetic cilia array surface with reversible deformation characteristics and excellent magnetic response performance, inspired by the ciliary structure of the human lung and its swinging pattern, as well as the behavior of pigeons using the geomagnetic field for directional migration [135]. The cilia's microscopic adhesion via van der Waals forces enables them to 'grip' solid microspheres underwater preventing slippage during directional transport. This adhesion-mediated control promotes precise drug targeting as the cilia maintain contact with the cargo until reaching the target site. Additionally, Shao et al. designed a microplate array (LS-MMA) integrating the characteristics of fish scales, Nepenthes, and respiratory cilia for multi-substance transport, as shown in Figure 16a [137]. Ben et al. developed a magnetically controlled super-wettable micro-cilia surface for droplet manipulation, overcoming the challenges of traditional methods, as shown in Figure 16c [134]. Jing et al. designed a magnetic micro-pillar array to achieve controllable manipulation of three-dimensional droplets, as shown in Figure 16b [115]. Kravanja et al. demonstrated an array of micro lamellae made of soft magnetic active elastomer for efficient droplet transport, as shown in Figure 16d [136]. These technologies enable precise control of droplet movement, realizing functions such as long-distance transport and obstacle crossing, which provides possibilities for targeted drug delivery and is expected to improve therapeutic effects while reducing side effects.

Compared to magnetically actuated biomimetic setal arrays, vibration-driven methods are considered a low-cost and efficient means of transport. Zhou and Cheng et al. developed a vibration-driven biomimetic array that enables bidirectional transport of objects under different vibration frequencies, as shown in the Figure 17 [140]. By leveraging the friction anisotropy of setae and their elastic deformation–energy release process during the vibration cycle, forward, backward, and directional transport of objects can be achieved. Moreover, based on experimental investigations and large deflection beam theory, Cheng et al. revealed that such setal arrays possess multistage load-bearing capabilities and effectively suppress frictional force fluctuations, thereby exhibiting high load-bearing capacity and transport stability [141–143].

Another major application in drug transport is bionic microneedle arrays [116, 144–151], as shown in Figure 18. Microneedles, an emerging drug delivery technology, achieve transdermal drug delivery by creating tiny pores on the skin surface, offering advantages such as painlessness and high efficiency. Integrating micro-nano structures with microneedle arrays enables efficient drug transport, and the schematic diagram is shown in Figure 18a [116]. For example, Zhu et al. designed an active injection microneedle patch inspired by the predatory behavior of blue-ringed octopuses, as shown in Figure 18c [149]. The patch mimics the octopu's ability to regulate adhesion via muscular control, its microneedles, coated with bioadhesive materials, form strong adhesion with tissue surfaces upon insertion, ensuring the three-stage "puncture-injection-maintenance" process proceeds without displacement. Body temperature triggers drug release from the tip cavity, while adhesion prevents detachment during the procedure, overcoming barriers of mucosal or skin permeability. Similarly, Song et al. combined octopus suction cup arrays with microneedle arrays to enhance skin adhesion, The suction cups generate negative pressure to secure the patch, while microneedles penetrate the stratum corneum [152]; together, these adhesion mechanisms ensure the array remains in place, improving drug delivery efficiency by minimizing gaps between the device and skin. Additionally, McKenna et al. developed polymer microneedle arrays

that successfully improved the transdermal delivery performance of olanzapine, as shown in Figure 18d [147], further expanding the applicability of bionic microneedles in addressing drug delivery challenges. Chen et al. meanwhile, prepared fully embeddable chitosan microneedles to serve as sustained-release depots for intradermal vaccination, as shown in Figure 18b [151], this highlights the key role of the technology in enhancing vaccine delivery efficiency and optimizing immune strategies. These chitosan microneedles exhibit favorable biodegradability in vivo. After being embedded in rat skin, histological observations show that they gradually degrade: significant degradation is observed at 1 week, and small residual fragments remain at the insertion site even after 14 days, with complete degradation within 21 days [151]. The degradation process is synchronized with antigen release: approximately 30% of the antigen is rapidly released in the initial 1–3 days due to fluid swelling, followed by gradual release of the remaining dose through enzymatic hydrolysis of chitosan from day 4 to day 14. This degradation cycle matches the immune response period, ensuring sustained antigen release during the critical window of immune cell activation (7–14 days) to enhance vaccine efficacy. The degradation products are non-toxic glucosamine, which is metabolized by the body without inducing adverse reactions, making them biocompatible and suitable for intradermal vaccination applications.

Overall, these studies, targeting different application scenarios, collectively demonstrate the innovative breakthroughs and broad application prospects of bionic microneedle arrays in efficient drug delivery and clinical therapy.

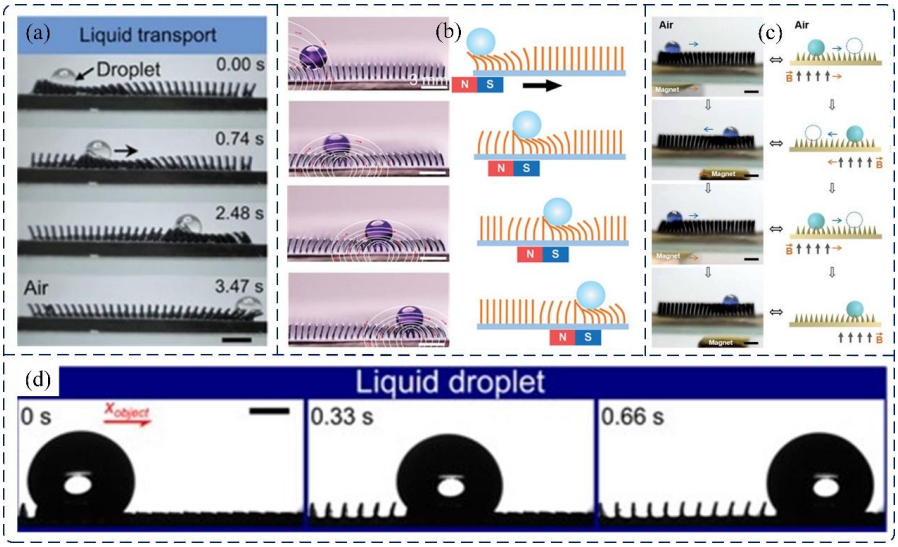



**Figure 16 Bio-inspired droplet transport based on array structures.**
(a) Images of droplet transport realized based on LS-MMA. Reproduced with permission. Shao K, Jiang S, Hu Y, et al. Bioinspired Lubricated Slippery Magnetic Responsive Microplate Array for High Performance Multi-Substance Transport. *Adv Funct Mater*. 2022;32(40):2205831. Copyright 2022, WILEY. (b) Schematic diagrams and optical images of droplet transport in the horizontal direction on the SMMA surface. Reproduced with permission. Jing X, Chen H, Zhang L, et al. Accurate Magneto-Driven Multi-Dimensional Droplet Manipulation. *Adv Funct Mater*. 2022;33(9):2210883. Copyright 2022, WILEY. (c) Schematic diagrams and optical images of the droplet transport process on the SMMA surface under an applied external magnetic field. Reproduced with permission. Ben S, Zhou T, Ma H, et al. Multifunctional Magnetocontrollable Superwettable-Microcilia Surface for Directional Droplet Manipulation. *Adv Sci*. 2019;6(17):1900834. Copyright 2019, WILEY. (d) Sequential images of liquid transport on the LM-MAS. Reproduced with permission. Kravanja G, Kriegl R, Hribar L, et al. Magnetically Actuated Surface Microstructures for Efficient Transport and Tunable Separation of Droplets and Solids. *Adv Eng Mater*. 2023;25(22):2301000. Copyright 2023, WILEY.

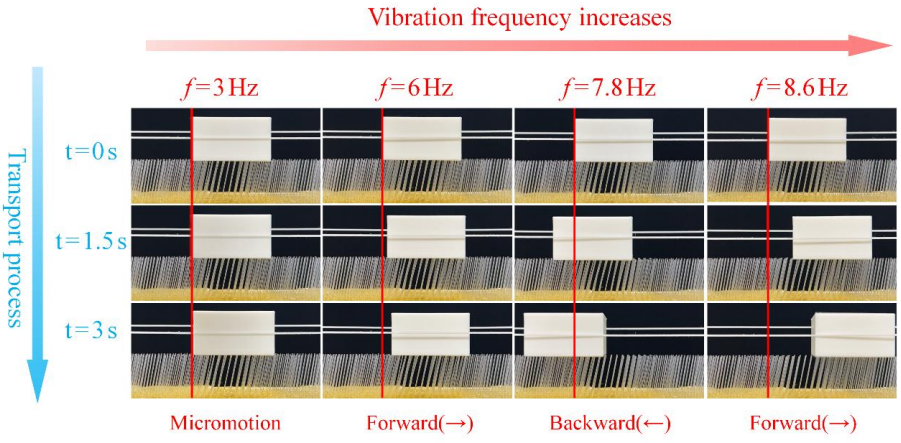



**Figure 17 Regulation of different transport directions under increasing vibration frequency.**
Reproduced with permission. Zhou Z, Liu T, Gu X, Zhu Z, Cheng Q, Jiang H. Bidirectional Object Transport on Biomimetic Setal Array with Friction Anisotropy. *Tribol Lett*. 2025;73(2):56. Copyright 2025, Springer Nature.

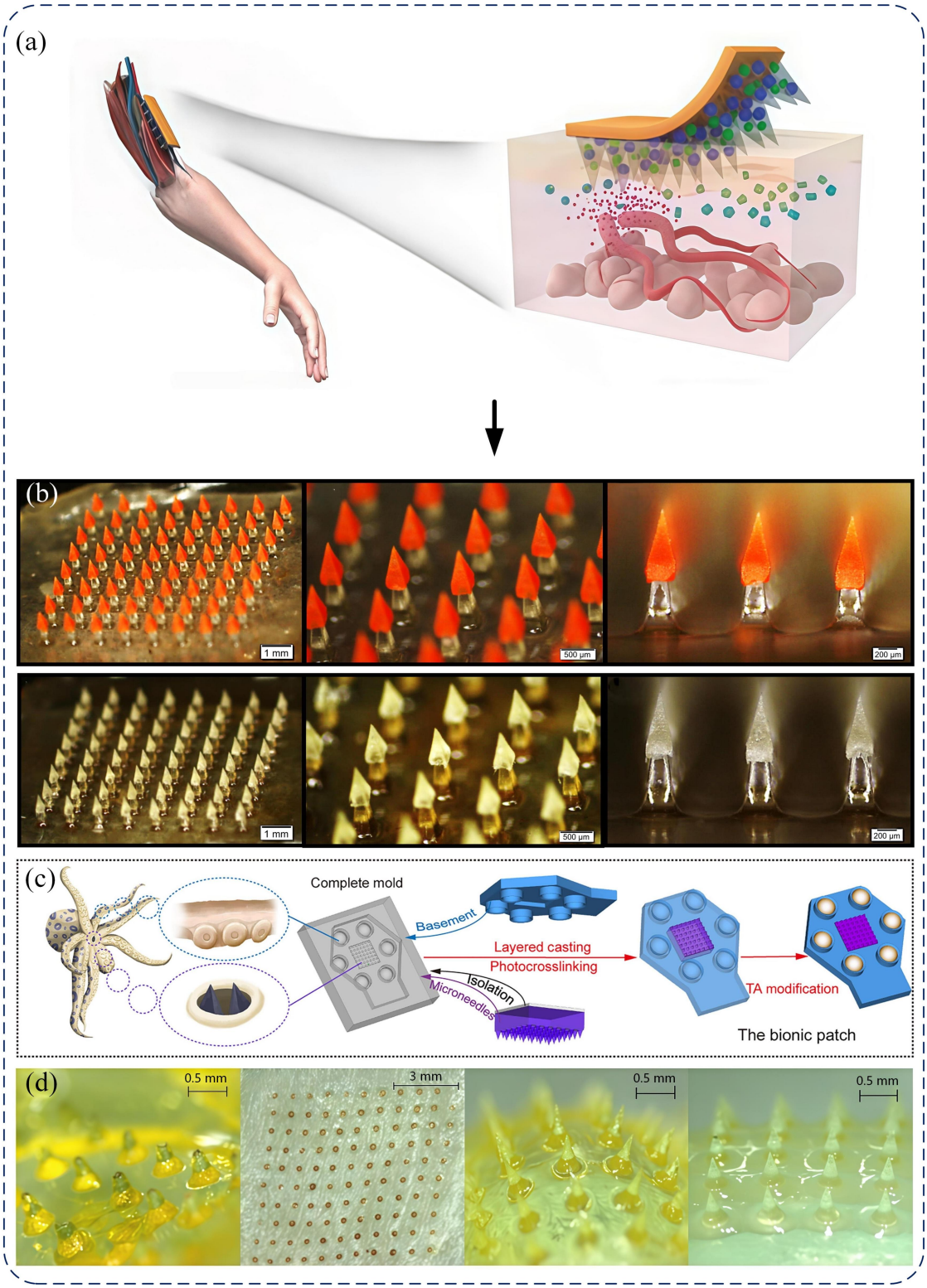



**Figure 18 Bioinspired microneedle patches for transdermal applications.**
(a) Schematic diagram of the microneedle patch. Reproduced with permission. Zhao L, Zhang C, Abu-Ershaid JM, et al. Smart Responsive Microarray Patches for Transdermal Drug Delivery and Biological Monitoring. *Adv Healthc Mater*. 2021;10(20):2100996. Copyright 2021, WILEY. (b) Microscopic image of drug-loaded microneedle array. Reproduced with permission. Chen MC, Huang SF, Lai KY, Ling MH. Fully embeddable chitosan microneedles as a sustained release depot for intradermal vaccination. *Biomaterials*. 2013;34(12):3077–3086. Copyright 2013, Elsevier. (c) Schematic diagram of a microneedle array patch inspired by the blue-ringed octopus. Reproduced with permission. Zhu Z, Wang J, Pei X, et al. Blue-ringed octopus-inspired microneedle patch for robust tissue surface adhesion and active injection drug delivery. *Sci Adv*. 2023;9(25):eadh2213. Copyright 2023, AAAS. (d) In vitro permeation test image of hydrogel microneedle array. Reproduced with permission. McKenna PE, Abbate MTA, Vora LK, et al. Polymeric Microarray Patches for Enhanced Transdermal Delivery of the Poorly Soluble Drug Olanzapine. *ACS Appl Mater Interfaces*. 2023;15(26):31300–31319. Copyright 2023, American Chemical Society.

Table 3 Drug delivery applications

| Scenarios | Inspiration | Design | References | Advantages |
|---|---|---|---|---|
| Transdermal | Octopus beetle | Micro-suckers/microcolumns | [8, 132] | Non-invasive stable |
| Targeted delivery | Octopus lung cilia | Magnetic cilia/plungers | [133, 135] | Precise stimulus-responsive |
| Minimally invasive | Blue-ringed octopus | Thermo-microneedles | [149, 151, 152] | Barrier-penetrating body-triggered |

Bionic adhesives offer new opportunities in the field of drug transport. By mimicking the diverse adhesion mechanisms of natural organisms such as the microstructured dry adhesion of geckos, the wet adhesion of tree frogs and mussels, and the suction-cup-based controllable adhesion of octopuses, drug delivery systems with enhanced adhesion strength, improved controlled release capabilities, and superior biocompatibility can be designed. These bioinspired systems not only address the limitations of traditional drug carriers such as poor interfacial adhesion in complex physiological environments and uncontrollable drug release kinetics but also enable targeted and sustained drug delivery, thereby optimizing therapeutic efficacy and reducing adverse effects.

Biomimetic adhesives in drug delivery face challenges that directly relate to adhesion performance. Some microneedle arrays may cause slight irritation due to excessive adhesion, reducing user compliance. Magnetic particles in targeted delivery systems must balance adhesion strength with biocompatibility, as their surface properties critical for both adhesion and metabolic safety require optimization. Additionally, the skin's natural barrier can weaken the adhesion of transdermal patches, even with microstructures, highlighting the need to refine adhesion mechanisms for enhanced interfacial contact. Addressing these issues requires tailoring adhesion strength to specific tissues, developing biocompatible materials with tunable stickiness, and integrating multi-scale structures to adapt to dynamic skin conditions.

## Emerging trends in biomimetic adhesives

In the landscape of biomimetic adhesives for biomedical engineering, while traditional dry and wet adhesion mechanisms have been well-explored, emerging trends such as enzyme-responsive adhesives and 4D-printed shape-memory adhesives are reshaping the future of the field.

Enzyme-responsive adhesives operate on the principle of modulating adhesion in response to specific enzymes present in biological environments. These adhesives contain chemical moieties or structures that are sensitive to enzymes. When encountering the target enzyme, the adhesive triggers a chemical reaction that either enhances or reduces its adhesiveness. For example, in a wound-healing context, as the wound progresses through different stages of healing, the concentration of certain enzymes changes. An enzyme-responsive adhesive can be designed to gradually lose its adhesion as the wound heals, minimizing damage to newly formed tissue during removal [153]. This property also makes them ideal candidates for targeted drug delivery systems. They can be engineered to release drugs precisely at the site where a specific enzyme is present, maximizing therapeutic efficacy while minimizing side-effects.

4D-printed shape-memory adhesives integrate the concepts of 4D printing and shape-memory materials. 4D printing adds a temporal dimension to traditional 3D printing, allowing printed objects to change their shape over time in response to environmental stimuli like temperature, pH, or moisture. Shape-memory adhesives can be programmed to have an initial shape. Once placed in a physiological environment, they transform into a different shape. In surgical applications, for instance, a 4D-printed shape-memory adhesive used for wound closure can conform to the changing shape of the wound during the healing process. It can provide consistent pressure to promote healing without causing excessive stress on the surrounding tissues [154]. This adaptability makes them highly promising for improving the effectiveness and safety of medical procedures.

These emerging adhesive technologies represent a significant step forward in biomimetic adhesives, offering solutions to the limitations of traditional adhesives in complex physiological environments and opening up new possibilities for medical innovation.

Although biomimetic adhesives hold broad application prospects in the biomedical field, their long-term biocompatibility as exogenous materials in vivo still faces critical challenges related to immune responses and tissue reactions. After synthetic adhesives are implanted in the body, their surfaces tend to rapidly adsorb proteins, triggering the aggregation of immune cells (such as macrophages) and the release of inflammatory factors, which may lead to local inflammation, fibrosis, or even foreign body rejection. This is particularly prominent in long-term implantation scenarios.

In addition, the matching between the degradation behavior of materials and the body's metabolism directly affects long-term safety. The degradation products of some synthetic adhesives may be cytotoxic or cause tissue damage due to excessively fast degradation rates; while incompletely degraded residues may continuously stimulate surrounding tissues and induce chronic immune responses. For example, synthetic polymer-based adhesives may undergo surface erosion in the body fluid environment, resulting in changes in microstructure, which in turn affects cell compatibility and tissue integration ability.

To address these challenges, research needs to proceed from both material design and immune regulation: reducing immunogenicity through chemical modification, or adopting degradable natural polymers to match the rhythm of physiological metabolism.

## Conclusions and outlook

This review systematically summarizes the research progress of biomimetic adhesives in biomedical engineering, covering aspects from micro/nano structure design to practical applications. Natural organisms such as geckos, tree frogs, and octopuses, with their unique micro/nano structures and adhesion mechanisms, have provided abundant inspiration for the design of biomimetic adhesives. Geckos rely on hierarchical setae arrays and van der Waals forces to achieve dry adhesion; tree frogs utilize hexagonal microcolumns and capillary action for wet adhesion; and octopuses achieve underwater adhesion through sucker arrays and negative pressure. These biological adhesion mechanisms have laid the foundation for the establishment of interfacial adhesion models, including solid-solid interface models such as the Johnson-Kendall-Roberts (JKR) contact model and Kendall peeling model, as well as solid-liquid-solid interface models such as the capillary model, suction cup model, and multiscale hierarchical models.

Guided by these models, researchers have designed diverse bioinspired adhesive structures, including setae arrays, polygonal pillar arrays, suction cup arrays, and hybrid architectures. These adhesives have shown broad application prospects in medical monitoring, soft tissue gripping, and drug delivery. In medical monitoring, they enhance the stability of wearable devices and implantable sensors in dynamic physiological environments. In soft tissue gripping, they reduce tissue damage in surgical procedures and promote wound healing. In drug delivery, they improve transdermal efficiency and targeted release capabilities.

However, current research still faces challenges, particularly in specific application scenarios that require further exploration. For long-term medical monitoring relying on wet adhesion, such as continuous ECG monitoring under sweating conditions or wound healing tracking in humid environments, several critical bottlenecks

exist. The core of wet adhesion relies on liquid bridges formed by capillary action or mucus-mediated interactions. During long-term use, physiological activities such as skin stretching, sweating, and sebum secretion may disrupt these liquid bridges, either by diluting the liquid medium, causing uneven distribution of capillary forces, or inducing premature detachment due to interfacial shear. For example, tree frog-inspired hexagonal microcolumn adhesives, while effective in short-term wet environments, often suffer from reduced contact area and adhesion strength after continuous skin contact, due to mucus drying or channel blockage by skin debris. Wet adhesives typically require hydrophilic materials to maintain liquid bridges, but these materials may cause skin maceration or allergic reactions under long-term occlusion. Additionally, residual adhesive components may trigger local inflammatory responses when in contact with damaged skin, limiting their applicability in chronic wound monitoring. In wearable sensors integrated with wet adhesives, the gradual weakening of adhesion can lead to micro-motion between the sensor and the skin, introducing noise into physiological signals. This issue is exacerbated in dynamic scenarios such as exercise, where periodic stress further accelerates adhesion fatigue.

To address these challenges, researchers are actively exploring new solutions. Hybrid structures combining tree frog-inspired drainage channels and octopus-like sucker arrays have shown promise. For instance, the tree frog-octopus hybrid patch retains hexagonal microcolumns to drain excess sweat while integrating micro-suckers to maintain negative pressure, reducing dependence on liquid bridges. Enzyme-responsive polymers are being incorporated into wet adhesives to dynamically regulate adhesion performance. By loading protease-sensitive linkers into the matrix, the adhesive can gradually reduce stickiness as wound healing progresses, avoiding tissue damage during removal. Similarly, 4D-printed shape-memory adhesives can respond to changes in skin temperature, adjusting surface roughness to re-engage with the skin during stretching and maintaining contact stability. Natural polymers such as hyaluronic acid and chitosan are replacing synthetic elastomers in wet adhesives to reduce skin irritation. Surface modification with anti-fouling peptides can further inhibit bacterial colonization and protein adsorption, preventing channel blockage and extending service life.

Beyond these specific challenges, broader issues remain. The stability and reliability of biomimetic adhesives under complex physiological conditions need further improvement. Biocompatibility and long-term safety require rigorous validation, especially for long-term implants, where immune responses and degradation byproducts may cause adverse effects. Large-scale manufacturing of high-precision micro/nano structures remains costly, hindering clinical translation. Emerging issues such as skin irritation caused by microneedles in drug delivery and insufficient adhesion of dry adhesives on wet tissues also need to be addressed.

Future research should focus on deepening the understanding of biological adhesion mechanisms and exploring new principles and models. Developing adhesives with enhanced environmental adaptability and intelligent responsiveness is crucial to meet diverse medical scenarios, such as designing wet adhesives with self-healing liquid bridges or stress-responsive surface topographies for long-term monitoring. Improving biocompatibility and biodegradability can facilitate clinical translation, while integrating advanced manufacturing technologies will enable precise design and scalable production of bioinspired structures. Exploring emerging trends such as enzyme-responsive adhesives and 4D-printed shape-memory adhesives can further expand the application scope of biomimetic adhesives.

In conclusion, bioinspired adhesives hold tremendous potential in biomedical engineering. Continued research will drive their innovative applications in healthcare, offering novel solutions for disease diagnosis, treatment, and prevention.

***References***

1. Arzt E, Gorb S, Spolenak R. From micro to nano contacts in biological attachment devices. *Proc Natl Acad Sci USA*. 2003;100(19):10603–10606. Available at: https://doi.org/10.1073/pnas.1534701100
2. Langowski JKA, Dodou D, van Assenbergh P, van Leeuwen JL. Design of Tree-Frog-Inspired Adhesives. *Integr Comp Biol*. 2020;60(4):906–918. Available at: https://doi.org/10.1093/icb/icaa037
3. Tramacere F, Beccai L, Kuba M, Gozzi A, Bifone A, Mazzolai B. The morphology and adhesion mechanism of octopus vulgaris suckers. *PLoS One*. 2013;8(6):e65074. Available at: https://doi.org/10.1371/journal.pone.0065074
4. Johnson KL, Kendall K, Roberts AD. Surface energy and the contact of elastic solids. *Proc R Soc Lond A*. 1971;324:301–313. Available at: https://doi.org/10.1098/rspa.1971.0141
5. Kendall K. Thin-film peeling-the elastic term. *J Phys D: Appl Phys*. 1975;8(13):1449–1452. Available at: https://doi.org/10.1088/0022-3727/8/13/005
6. Butt HJ, Kappl M. Normal capillary forces. *Adv Colloid Interface Sci*. 2009;146(1–2):48–60. Available at: https://doi.org/10.1016/j.cis.2008.10.002
7. Orr FM, Scriven LE, Rivas AP. Pendular rings between solids: meniscus properties and capillary force. *J Fluid Mech*. 1975;67(4):723–742. Available at: https://doi.org/10.1017/S0022112075000572
8. Choi MK, Park OK, Choi C, et al. Cephalopod-Inspired Miniaturized Suction Cups for Smart Medical Skin. *Adv Healthc Mater*. 2016;5(1):80–87. Available at: https://doi.org/10.1002/adhm.201500285
9. Drotlef D, Amjadi M, Yunusa M, Sitti M. Bioinspired Composite Microfibers for Skin Adhesion and Signal Amplification of Wearable Sensors. *Adv Mater*. 2017;29(28):1701353. Available at: https://doi.org/10.1002/adma.201701353
10. Mahdavi A, Ferreira L, Sundback C, et al. A biodegradable and biocompatible gecko-inspired tissue adhesive. *Proc Natl Acad Sci USA*. 2008;105(7):2307–2312. Available at: https://doi.org/doi:10.1073/pnas.0712117105
11. Song JH, Baik S, Kim DW, Yang TH, Pang C. Wet soft bio-adhesion of insect-inspired polymeric oil-loadable perforated microcylinders. *Chem Eng J*. 2021;423:130194. Available at: https://doi.org/10.1016/j.cej.2021.130194
12. Huang R, Zhang X, Li W, Shang L, Wang H, Zhao Y. Suction Cups-Inspired Adhesive Patch with Tailorable Patterns for Versatile Wound Healing. *Adv Sci*. 2021;8(17):2100201. Available at: https://doi.org/10.1002/advs.202100201
13. Tian Y, Pesika N, Zeng H, et al. Adhesion and friction in gecko toe attachment and detachment. *Proc Natl Acad Sci USA*. 2006;103(51):19320–19325. Available at https://doi.org/10.1073/pnas.0608841103
14. Autumn K, Liang YA, Hsieh ST, et al. Adhesive force of a single gecko foot-hair. *Nature*. 2000;405(6787):681–685. Available at: https://doi.org/10.1038/35015073
15. Hamaker HC. The London—van der Waals attraction between spherical particles. *Physica*. 1937;4(10):1058–1072. Available at: https://doi.org/10.1016/S0031-8914(37)80203-7
16. Majumder A, Sharma A, Ghatak A. Bio-Inspired Adhesion and Adhesives: Controlling Adhesion by Micro-Nano Structuring of Soft Surfaces. *Microfluidics and Microfabrication November*. 2009:283–307. Available at: https://doi.org/10.1007/978-1-4419-1543-6_7
17. Lake GJ, Thomas AG. The strength of highly elastic materials.

*Proc R Soc Lond A*. 1967;300(1460):108–119. Available at: https://doi.org/10.1098/rspa.1967.0160
18. Gao H, Yao H. Shape insensitive optimal adhesion of nanoscale fibrillar structures. *Proc Natl Acad Sci USA*. 2004;101(21):7851–7856. Available at: https://doi.org/10.1073/pnas.0400757101
19. Kamperman M, Kroner E, del Campo A, McMeeking RM, Arzt E. Functional Adhesive Surfaces with "Gecko" Effect: The Concept of Contact Splitting. *Adv Eng Mater*. 2010;12(5):335–348. Available at: https://doi.org/10.1002/adem.201000104
20. Gao H, Wang X, Yao H, Gorb S, Arzt E. Mechanics of hierarchical adhesion structures of geckos. *Mech Mater*. 2005;37(2–3):275–285. Available at: https://doi.org/10.1016/j.mechmat.2004.03.008
21. Peisker H, Michels J, Gorb SN. Evidence for a material gradient in the adhesive tarsal setae of the ladybird beetle Coccinella septempunctata. *Nat Commun*. 2013;4:1661. Available at: https://doi.org/10.1038/ncomms2576
22. Borodich FM, Savencu O. Hierarchical Models of Engineering Rough Surfaces and Bio-inspired Adhesives. *Biologically-Inspired Systems*. 2017:179–219. Available at: https://doi.org/10.1007/978-3-319-59114-8_10
23. Heepe L, Gorb SN. Biologically Inspired Mushroom-Shaped Adhesive Microstructures. *Annu Rev Mater Res*. 2014;44:173–203. Available at: https://doi.org/10.1146/annurev-matsci-062910-100458
24. Murarash B, Itovich Y, Varenberg M. Tuning elastomer friction by hexagonal surface patterning. *Soft Matter*. 2011;7(12):5553–5557. Available at: https://doi.org/10.1039/C1SM00015B
25. Drotlef D, Stepien L, Kappl M, Barnes WJP, Butt H, del Campo A. Insights into the Adhesive Mechanisms of Tree Frogs using Artificial Mimics. *Adv Funct Mater*. 2013;23(9):1137–1146. Available at: https://doi.org/10.1002/adfm.201202024
26. Seol JU, Park JS, Lim JH, et al. Dynamic mucus secretion in ventral surfaces of toe pads of the tree frog (Dryophytes japonica). *Integr Zool*. 2024;19(6):1076–1091. Available at: https://doi.org/10.1111/1749-4877.12821
27. Borodich FM, Gorb EV, Gorb SN. Fracture behaviour of plant epicuticular wax crystals and its role in preventing insect attachment: a theoretical approach. *Appl Phys A*. 2010;100:63–71. Available at: https://doi.org/10.1007/s00339-010-5794-x
28. Borodich FM, Gao Z, Gorb EV, Gorb SN, Jin X. Wax Protrusions on Anti-Adhesive Plant Surfaces and Their Interactions with Insect Adhesive Pads: A Mechanical Interpretation. *Biomimetics*. 2024;9(7):442. Available at: https://doi.org/10.3390/biomimetics9070442
29. Lee H, Um D, Lee Y, Lim S, Kim H, Ko H. Octopus-Inspired Smart Adhesive Pads for Transfer Printing of Semiconducting Nanomembranes. *Adv Mater*. 2016;28(34):7457–7465. Available at: https://doi.org/10.1002/adma.201601407
30. Tan T, Yu L, Guo K, Wang X, Qiao L. Biomimetic Robotic Remora With Hitchhiking Ability: Design, Control and Experiment. *IEEE Robot Autom Lett*. 2024;9(12):11505–11512. Available at: https://doi.org/10.1109/lra.2024.3487075
31. Wang S, Li L, Zhao W, Zhang Y, Wen L. A biomimetic remora disc with tunable, reversible adhesion for surface sliding and skimming. *Bioinspir Biomim*. 2022;17(3):036001. Available at: https://doi.org/10.1088/1748-3190/ac4e7a
32. Wang Y, Yang X, Chen Y, et al. A biorobotic adhesive disc for underwater hitchhiking inspired by the remora suckerfish. *Sci Robot*. 2017;2(10):eaan8072. Available at: https://doi.org/10.1126/scirobotics.aan8072
33. Wang J, Wang S, Zheng L, Ren L. Adhesion Behavior in Fish: From Structures to Applications. *Biomimetics*. 2023;8(7):534. Available at: https://doi.org/10.3390/biomimetics8070534
34. Gamel KM, Garner AM, Flammang BE. Bioinspired remora adhesive disc offers insight into evolution. *Bioinspir Biomim*. 2019;14(5):056014. Available at: https://doi.org/10.1088/1748-3190/ab3895
35. Wang S, Li L, Sun W, et al. Detachment of the remora suckerfish disc: kinematics and a bio-inspired robotic model. *Bioinspir Biomim*. 2020;15(5):056018. Available at: https://doi.org/10.1088/1748-3190/ab9418
36. Lee SH, Song HW, Kang BS, Kwak MK. Remora-Inspired Reversible Adhesive for Underwater Applications. *ACS Appl Mater Interfaces*. 2019;11(50):47571–47576. Available at: https://doi.org/10.1021/acsami.9b16350
37. Su S, Wang S, Li L, et al. Vertical Fibrous Morphology and Structure-Function Relationship in Natural and Biomimetic Suction-Based Adhesion Discs. *Matter*. 2020;2(5):1207–1221. Available at: https://doi.org/10.1016/j.matt.2020.01.018
38. Guo Y, Wang X, Zhang L, et al. From Dry to Wet, the Nature Inspired Strong Attachment Surfaces and Their Medical Applications. *ACS Nano*. 2025;19(10):9684–9708. Available at: https://doi.org/10.1021/acsnano.4c17864
39. Kier WM, Smith AM. The Structure and Adhesive Mechanism of Octopus Suckers. *Integr Comp Biol*. 2002;42(6):1146–1153. Available at: https://doi.org/10.1093/icb/42.6.1146
40. Kier WM, Smith AM. The Morphology and Mechanics of Octopus Suckers. *Biol Bull*. 1990;178(2):126–136. Available at: https://doi.org/10.2307/1541971
41. Tiwari A, Dorogin L, Tahir M, et al. Rubber contact mechanics: adhesion, friction and leakage of seals. *Soft Matter*. 2017;13(48):9103–9121. Available at: https://doi.org/10.1039/c7sm02038d
42. Arzt E, Quan H, McMeeking RM, Hensel R. Functional surface microstructures inspired by nature – From adhesion and wetting principles to sustainable new devices. *Prog Mater Sci*. 2021;120:100823. Available at: https://doi.org/10.1016/j.pmatsci.2021.100823
43. Tramacere F, Pugno NM, Kuba MJ, Mazzolai B. Unveiling the morphology of the acetabulum in octopus suckers and its role in attachment. *Interface Focus*. 2015;5(1):20140050. Available at: https://doi.org/10.1098/rsfs.2014.0050
44. Wang Y, Li Z, Elhebeary M, Hensel R, Arzt E, Saif MTA. Water as a "glue": Elasticity-enhanced wet attachment of biomimetic microcup structures. *Sci Adv*. 2022;8(12):eabm9341. Available at: https://doi.org/10.1126/sciadv.abm9341
45. Baik S, Kim DW, Park Y, Lee TJ, Bhang SH, Pang C. A wet-tolerant adhesive patch inspired by protuberances in suction cups of octopi. *Nature*. 2017;546(7658):396–400. Available at: https://doi.org/10.1038/nature22382
46. Derjaguin B. Untersuchungen über die Reibung und Adhäsion, IV. *Kolloid-Z*. 1934;69(2):155–164. Available at: https://doi.org/10.1007/BF01433225
47. Greenwood JA. Adhesion of elastic spheres. *Proc R Soc Lond A*. 1997;453(1961):1277–1297. Available at: https://doi.org/10.1098/rspa.1997.0070
48. Borodich FM. The Hertz-Type and Adhesive Contact Problems for Depth-Sensing Indentation. *Adv Appl Mech*. 2014;47:225–366. Available at: https://doi.org/10.1016/B978-0-12-800130-1.00003-5
49. Bradley RS. The cohesive force between solid surfaces and the surface energy of solids. *The London, Edinburgh, and Dublin Philosophical Magazine and Journal of Science*. 1932;13(86):853-862. Available at: https://doi.org/10.1080/14786449209461990

50. Sperling G. Eine Theorie der Haftung von Feststoffteilchen an festen Körpen (Unpublished doctoral dissertation). Technische Hochschule Karlsruhe. 1964. Available at: https://www.researchgate.net/publication/35428591
51. Kendall K. Molecular adhesion and its applications: the sticky universe. *New York: Kluwer Academic/Plenum Publishers* 2001:429. Available at: https://doi.org/10.1007/b100328
52. Scherge M, Gorb S. Biological micro- and nanotribology: nature's solutions. *Springer Berlin Heidelberg*. 2001. Available at: https://doi.org/10.1007/978-3-662-04431-5
53. Borodich FM, Galanov BA, Suarez-Alvarez MM. The JKR-type adhesive contact problems for power-law shaped axisymmetric punches. *J Mech Phys Solids.* 2014;68:14–32. Available at: https://doi.org/10.1016/j.jmps.2014.03.003
54. Cheng Q, Jiang Z, Borodich FM, Gorb SN, Jin X. Interaction of a non-axisymmetric artificial single spatula with rough surfaces. *Interface Focus.* 2024;14(3):20230081. Available at: https://doi.org/10.1098/rsfs.2023.0081
55. Vishnubhotla SB, Chen R, Khanal SR, Hu X, Martini A, Jacobs TDB. Matching Atomistic Simulations and In Situ Experiments to Investigate the Mechanics of Nanoscale Contact. *Tribol Lett.* 2019;67(3):97. Available at: https://doi.org/10.1007/s11249-019-1210-7
56. Li Y, Zhang J, Zhang Y, Zhao M, Lu C, Liu M. A semi-analytical solution for determining plastic parameters of metallic materials from scratch tests. *Int J Solids Struct.* 2025;310:113226. Available at: https://doi.org/10.1016/j.ijsolstr.2025.113226
57. Zhou YT, Kim TW. Role of rough surface on contact between magneto-electro-elastic materials and orthotropic solid. *Int J Mech Sci.* 2015;99:187–195. Available at: https://doi.org/10.1016/j.ijmecsci.2015.05.017
58. Butt HJ, Graf K, Kappl M. Liquid Surfaces. *Physics and Chemistry of Interfaces*. 2003;2:4–25. Available at: https://doi.org/10.1002/3527602313.ch2
59. Langowski JKA, Dodou D, Kamperman M, van Leeuwen JL. Tree frog attachment: mechanisms, challenges, and perspectives. *Front Zool.* 2018;15:32. Available at: https://doi.org/10.1186/s12983-018-0273-x
60. Barnes WJ, Baum M, Peisker H, Gorb SN. Comparative Cryo-SEM and AFM studies of hylid and rhacophorid tree frog toe pads. *J Morphol.* 2013;274(12):1384–1396. Available at: https://doi.org/10.1002/jmor.20186
61. Scholz I, Barnes WJP, Smith JM, Baumgartner W. Ultrastructure and physical properties of an adhesive surface, the toe pad epithelium of the tree frog, Litoria caerulea White. *J Exp Biol.* 2009;212(2):155–162. Available at: https://doi.org/10.1242/jeb.019232
62. Archard J. Elastic deformation and the laws of friction. *Proc R Soc Lond A*. 1957;243(1233):190–205. Available at: https://doi.org/10.1098/rspa.1957.0214
63. Borodich FM, Gao Z, Jin X. Fractal models in tribology: A critical review. *Friction.* 2025;13(4):9440945. Available at: https://doi.org/10.26599/FRICT.2025.9440945
64. Liu SH. Fractal model for the ac response of a rough interface. *Phys Rev Lett.* 1985;55(5):529–532. Available at: https://doi.org/10.1103/PhysRevLett.55.529
65. Borodich FM, Mosolov AB. Fractal roughness in contact problems. *J Appl Math Mech*. 1992;56(5):681–690. Available at: https://doi.org/10.1016/0021-8928(92)90054-C
66. Borodich FM, Mosolov AB. Fractal contact of solids. *JZhurnal Tekhnicheskoi Fiziki.* 1991;61(9):50–54. Available at: https://www.mathnet.ru/eng/jtf4400
67. Cheng Q, Borodich FM, Gao Z, Gorb SN, Jin X. Advances in the contact mechanics theory and applications of biomimetic artificial adhesives inspired by biological multiscale hierarchical structures. *Friction.* 2025;13:9441016. Available at: https://doi.org/10.26599/FRICT.2025.9441016
68. Plesha ME, Ni D. Scaling of geological discontinuity normal load–deformation response using fractal geometry. *Num Anal Meth Geomechanics.* 2001;25(8):741–756. Available at: https://doi.org/10.1002/nag.149
69. Warren TL, Krajcinovic D. Fractal models of elastic-perfectly plastic contact of rough surfaces based on the Cantor set. *Int J Solids Struct.* 1995;32(19):2907–2922. Available at: https://doi.org/10.1016/0020-7683(94)00241-N
70. Schmittbuhl J, Vilotte J, Roux S. Velocity weakening friction: A renormalization approach. *J Geophys Res.* 1996;101(B6):13911–13917. Available at: https://doi.org/10.1029/96JB00653
71. Tian Y, Wan J, Pesika N, Zhou M. Bridging nanocontacts to macroscale gecko adhesion by sliding soft lamellar skin supported setal array. *Sci Rep.* 2013;3:1382. Available at: https://doi.org/10.1038/srep01382
72. Borodich FM, Onishchenko DA. Similarity and fractality in the modelling of roughness by a multilevel profile with hierarchical structure. *Int J Solids Struct.* 1999;36(17):2585–2612. Available at: https://doi.org/10.1016/S0020-7683(98)00116-4
73. Borodich FM, Onishchenko DA. Fractal roughness in friction and contact problems (simplest models). *Journal of Friction and Wear*. 1993;14(3):14-19. Available at: https://www.researchgate.net/publication/280138041
74. Almuramady N, Borodich FM, Goryacheva IG, Torskaya EV. Damage of functionalized self-assembly monomolecular layers applied to silicon microgear MEMS. *Tribol Int.* 2019;129:202–213. Available at: https://doi.org/10.1016/j.triboint.2018.07.049
75. Gorb S. Attachment devices of insect cuticle. 2001. Available at: https://doi.org/10.1007/0-306-47515-4
76. Autumn K. Gecko Adhesion: Structure, Function, and Applications. *MRS Bull.* 2007;32(6):473–478. Available at: https://doi.org/10.1557/mrs2007.80
77. Gorb SN. Biological fibrillar adhesives: functional principles and biomimetic applications. *Handbook of Adhesion Technology*. 2011:1409–1436. Available at: https://doi.org/10.1007/978-3-642-01169-6_54
78. Spolenak R, Gorb S, Gao H, Arzt E. Effects of contact shape on the scaling of biological attachments. *Proc R Soc A.* 2005;461(2054):305–319. Available at: https://doi.org/10.1098/rspa.2004.1326
79. del Campo A, Greiner C, Arzt E. Contact Shape Controls Adhesion of Bioinspired Fibrillar Surfaces. *Langmuir.* 2007;23(20):10235–10243. Available at: https://doi.org/10.1021/la7010502
80. Greiner C, Spolenak R, Arzt E. Adhesion design maps for fibrillar adhesives: The effect of shape. *Acta Biomater.* 2009;5(2):597–606. Available at: https://doi.org/10.1016/j.actbio.2008.09.006
81. Niederegger S, Gorb S. Tarsal movements in flies during leg attachment and detachment on a smooth substrate. *J Insect Physiol.* 2003;49(6):611–620. Available at: https://doi.org/10.1016/s0022-1910(03)00048-9
82. Niederegger S, Gorb SN. Friction and adhesion in the tarsal and metatarsal scopulae of spiders. *J Comp Physiol A.* 2006;192(11):1223–1232. Available at: https://doi.org/10.1007/s00359-006-0157-y
83. Autumn K, Dittmore A, Santos D, Spenko M, Cutkosky M. Frictional adhesion: a new angle on gecko attachment. *J Exp Biol.* 2006;209(18):3569–3579. Available at: https://doi.org/10.1242/jeb.02486
84. Pesika NS, Tian Y, Zhao B, et al. Peel-Zone Model of Tape Peeling Based on the Gecko Adhesive System. *The Journal of Adhesion.* 2007;83(4):383–401. Available at: https://doi.org/10.1080/00218460701282539
85. Pugno NM. The theory of multiple peeling. *Int J Fract.* 2011;171(2):185–193. Available at:

https://doi.org/10.1007/s10704-011-9638-2
86. Carbone G, Pierro E. Sticky Bio-inspired Micropillars: Finding the Best Shape. *Small.* 2012;8(9):1449–1454. Available at: https://doi.org/10.1002/smll.201102021
87. Song S, Sitti M. Soft Grippers Using Micro-fibrillar Adhesives for Transfer Printing. *Adv Mater.* 2014;26(28):4901–4906. Available at: https://doi.org/10.1002/adma.201400630
88. Davies J, Haq S, Hawke T, Sargent JP. A practical approach to the development of a synthetic Gecko tape. *Int J Adhes Adhes.* 2009;29(4):380–390. Available at: https://doi.org/10.1016/j.ijadhadh.2008.07.009
89. Murphy MP, Aksak B, Sitti M. Gecko-Inspired Directional and Controllable Adhesion. *Small.* 2009;5(2):170–175. Available at: https://doi.org/10.1002/smll.200801161
90. Lin Q, Gourdon D, Sun C, et al. Adhesion mechanisms of the mussel foot proteins mfp-1 and mfp-3. *Proc Natl Acad Sci USA.* 2007;104(10):3782–3786. Available at: https://doi.org/10.1073/pnas.0607852104
91. Pelletier Y, Smilowitz Z. Specialized tarsal hairs on adult male colorado potato beetles, leptinotarsa decemlineata (say), hamper its locomotion on smooth surfaces. *Can Entomol.* 1987;119(12):1139–1142. Available at: https://doi.org/10.4039/Ent1191139-12
92. Stork NE. A comparison of the adhesive setae on the feet of lizards and arthropods. *J Nat Hist.* 1983;17(6):829–835. Available at: https://doi.org/10.1080/00222938300770641
93. Gorb SN, Varenberg M. Mushroom-shaped geometry of contact elements in biological adhesive systems. *J Adhes Sci Technol.* 2007;21(12–13):1175–1183. Available at: https://doi.org/10.1163/156856107782328317
94. Huber G, Gorb SN, Spolenak R, Arzt E. Resolving the nanoscale adhesion of individual gecko spatulae by atomic force microscopy. *Biol Lett.* 2005;1(1):2–4. Available at: https://doi.org/doi:10.1098/rsbl.2004.0254
95. Gorb S, Varenberg M, Peressadko A, Tuma J. Biomimetic mushroom-shaped fibrillar adhesive microstructure. *J R Soc Interface.* 2007;4(13):271–275. Available at: https://doi.org/10.1098/rsif.2006.0164
96. Kovalev AE, Varenberg M, Gorb SN. Wet versus dry adhesion of biomimetic mushroom-shaped microstructures. Soft Matter. 2012;8(29):7560–7566. Available at: https://doi.org/10.1039/C2SM25431J
97. Varenberg M, Gorb S. A beetle-inspired solution for underwater adhesion. *J R Soc Interface.* 2008;5(20):383–385. Available at: https://doi.org/doi:10.1098/rsif.2007.1171
98. Linghu C, Zhang S, Wang C, Song J. Transfer printing techniques for flexible and stretchable inorganic electronics. *npj Flex Electron.* 2018;2:26. Available at: https://doi.org/10.1038/s41528-018-0037-x
99. Chen H, Zhang L, Zhang D, Zhang P, Han Z. Bioinspired Surface for Surgical Graspers Based on the Strong Wet Friction of Tree Frog Toe Pads. *ACS Appl Mater Interfaces.* 2015;7(25):13987–13995. Available at: https://doi.org/10.1021/acsami.5b03039
100. Iturri J, Xue L, Kappl M, et al. Torrent Frog-Inspired Adhesives: Attachment to Flooded Surfaces. *Adv Funct Mater.* 2015;25(10):1499–1505. Available at: https://doi.org/10.1002/adfm.201403751
101. Xie J, Li M, Dai Q, Huang W, Wang X. Key parameters of biomimetic patterned surface for wet adhesion. *Int J Adhes Adhes.* 2018;82:72–78. Available at: https://doi.org/10.1016/j.ijadhadh.2018.01.004
102. Gupta R, Fréchette J. Measurement and Scaling of Hydrodynamic Interactions in the Presence of Draining Channels. *Langmuir.* 2012;28(41):14703–14712. Available at: https://doi.org/10.1021/la303508x
103. Tramacere F, Appel E, Mazzolai B, Gorb SN. Hairy suckers: the surface microstructure and its possible functional significance in the Octopus vulgaris sucker. *Beilstein J Nanotechnol.* 2014;5:561–565. Available at: https://doi.org/10.3762/bjnano.5.66
104. Britz R, Johnson GD. Ontogeny and homology of the skeletal elements that form the sucking disc of remoras (Teleostei, Echeneoidei, Echeneidae). *J Morphol.* 2012;273(12):1353–1366. Available at: https://doi.org/10.1002/jmor.20063
105. Culler M, Ledford KA, Nadler JH. The Role of Topology and Tissue Mechanics in Remora Attachment. *MRS Proc.* 2014;1648:102. Available at: https://doi.org/10.1557/opl.2014.229
106. Li M, Mao A, Guan Q, Saiz E. Nature-inspired adhesive systems. *Chem Soc Rev.* 2024;53(16):8240–8305. Available at: https://doi.org/10.1039/d3cs00764b
107. Baik S, Kim J, Lee HJ, Lee TH, Pang C. Highly Adaptable and Biocompatible Octopus-Like Adhesive Patches with Meniscus-Controlled Unfoldable 3D Microtips for Underwater Surface and Hairy Skin. *Adv Sci.* 2018;5(8):1800100. Available at: https://doi.org/10.1002/advs.201800100
108. Smith AM. Cephalopod Sucker Design and the Physical Limits to Negative Pressure. *J Exp Biol.* 1996;199(4):949–958. Available at: https://doi.org/10.1242/jeb.199.4.949
109. Lee H, Lee BP, Messersmith PB. A reversible wet/dry adhesive inspired by mussels and geckos. *Nature.* 2007;448(7151):338–341. Available at: https://doi.org/10.1038/nature05968
110. Dayan CB, Chun S, Krishna-Subbaiah N, Drotlef D, Akolpoglu MB, Sitti M. 3D Printing of Elastomeric Bioinspired Complex Adhesive Microstructures. *Adv Mater.* 2021;33(40):e2103826. Available at: https://doi.org/10.1002/adma.202103826
111. Kim DW, Baik S, Min H, et al. Highly Permeable Skin Patch with Conductive Hierarchical Architectures Inspired by Amphibians and Octopi for Omnidirectionally Enhanced Wet Adhesion. *Adv Funct Mater.* 2019;29(13):1807614. Available at: https://doi.org/10.1002/adfm.201807614
112. Linghu C, Wang C, Cen N, Wu J, Lai Z, Song J. Rapidly tunable and highly reversible bio-inspired dry adhesion for transfer printing in air and a vacuum. *Soft Matter.* 2019;15(1):30–37. Available at: https://doi.org/10.1039/C8SM01996G
113. Zhang L, Chen H, Guo Y, et al. Micro–Nano Hierarchical Structure Enhanced Strong Wet Friction Surface Inspired by Tree Frogs. *Adv Sci.* 2020;7(20):2001125. Available at: https://doi.org/10.1002/advs.202001125
114. Hoang TT, Quek JJS, Thai MT, Phan PT, Lovell NH, Do TN. Soft robotic fabric gripper with gecko adhesion and variable stiffness. *Sens Actuators A.* 2021;323:112673. Available at: https://doi.org/10.1016/j.sna.2021.112673
115. Jing X, Chen H, Zhang L, et al. Accurate Magneto-Driven Multi-Dimensional Droplet Manipulation. *Adv Funct Mater.* 2022;33(9):2210883. Available at: https://doi.org/10.1002/adfm.202210883
116. Zhao L, Zhang C, Abu-Ershaid JM, et al. Smart Responsive Microarray Patches for Transdermal Drug Delivery and Biological Monitoring. *Adv Healthc Mater.* 2021;10(20):2100996. Available at: https://doi.org/10.1002/adhm.202100996
117. Stauffer F, Thielen M, Sauter C, et al. Skin Conformal Polymer Electrodes for Clinical ECG and EEG Recordings. *Adv Healthc Mater.* 2018;7(7):1700994. Available at: https://doi.org/10.1002/adhm.201700994
118. Kim T, Park J, Sohn J, Cho D, Jeon S. Bioinspired, Highly Stretchable, and Conductive Dry Adhesives Based on 1D–2D Hybrid Carbon Nanocomposites for All-in-One ECG Electrodes.

*ACS Nano.* 2016;10(4):4770–4778. Available at: https://doi.org/10.1021/acsnano.6b01355
119. Kwak MK, Jeong H, Suh KY. Rational Design and Enhanced Biocompatibility of a Dry Adhesive Medical Skin Patch. *Adv Mater.* 2011;23(34):3949–3953. Available at: https://doi.org/10.1002/adma.201101694
120. Hwang I, Kim HN, Seong M, et al. Multifunctional Smart Skin Adhesive Patches for Advanced Health Care. *Adv Healthc Mater.* 2018;7(15):1800275. Available at: https://doi.org/10.1002/adhm.201800275
121. Wang X, Sun X, Gan D, et al. Bioadhesive and conductive hydrogel-integrated brain-machine interfaces for conformal and immune-evasive contact with brain tissue. *Matter.* 2022;5(4):1204–1223. Available at: https://doi.org/10.1016/j.matt.2022.01.012
122. Lan T, Tian H, Chen X, et al. Treefrog-Inspired Flexible Electrode with High Permeability, Stable Adhesion, and Robust Durability. *Adv Mater.* 2024;36(31):2404761. Available at: https://doi.org/10.1002/adma.202404761
123. Lee YS, Kang GR, Kim MS, Kim DW, Pang C. Softened double-layer octopus-like adhesive with high adaptability for enhanced dynamic dry and wet adhesion. *Chem Eng J.* 2023;468:143792. Available at: https://doi.org/10.1016/j.cej.2023.143792
124. Wu X, Deng J, Jian W, et al. A bioinspired switchable adhesive patch with adhesion and suction mechanisms for laparoscopic surgeries. *Mater Today Bio.* 2024;27:101142. Available at: https://doi.org/10.1016/j.mtbio.2024.101142
125. Ahmad NN, Ghazali NNN, Rani ATA, Kee CC, Wong YH. Bioinspired adhesive patch with octopus vulgaris micro-sucker and hexagonal tree-frog pad structures. *Mater Sci Semicond Process.* 2023;166:107731. Available at: https://doi.org/10.1016/j.mssp.2023.107731
126. Alizadehyazdi V, Bonthron M, Spenko M. An Electrostatic/Gecko-Inspired Adhesives Soft Robotic Gripper. *IEEE Robot Autom Lett.* 2020;5(3):4679–4686. Available at: https://doi.org/10.1109/LRA.2020.3003773
127. Tian Y, Zhang Q, Cai D, Chen C, Zhang J, Duan W. Theoretical modelling of soft robotic gripper with bioinspired fibrillar adhesives. *Mech Adv Mater Struct.* 2021;29(15):2250–2266. Available at: https://doi.org/10.1080/15376494.2020.1857482
128. Lee Y, Chun S, Son D, Hu X, Schneider M, Sitti M. A Tissue Adhesion-Controllable and Biocompatible Small-Scale Hydrogel Adhesive Robot. *Adv Mater.* 2022;34(13):2109325. Available at: https://doi.org/10.1002/adma.202109325
129. Jia B, Huang H, Dong Z, et al. Degradable biomedical elastomers: paving the future of tissue repair and regenerative medicine. *Chem Soc Rev.* 2024;53(8):4086–4153. Available at: https://doi.org/10.1039/D3CS00923H
130. Zhang X, Chen G, Yu Y, Sun L, Zhao Y. Bioinspired Adhesive and Antibacterial Microneedles for Versatile Transdermal Drug Delivery. *Research.* 2020:3672120. Available at: https://doi.org/10.34133/2020/3672120
131. Li W, Zheng Y, Pang W, Lai P. Bio-inspired adhesive hydrogel for wound healing. *Biomed Technol.* 2023;1:65–72. Available at: https://doi.org/10.1016/j.bmt.2022.11.009
132. Tsai CY, Chang CC. Auto-adhesive transdrermal drug delivery patches using beetle inspired micropillar structures. *J Mater Chem B.* 2013;1(43):5963–5970. Available at: https://doi.org/10.1039/c3tb20735h
133. Baik S, Lee J, Jeon EJ, et al. Diving beetle–like miniaturized plungers with reversible, rapid biofluid capturing for machine learning–based care of skin disease. *Sci Adv.* 2021;7(25):eabf5695. Available at: https://doi.org/10.1126/sciadv.abf5695
134. Ben S, Zhou T, Ma H, et al. Multifunctional Magnetocontrollable Superwettable-Microcilia Surface for Directional Droplet Manipulation. *Adv Sci.* 2019;6(17):1900834. Available at: https://doi.org/10.1002/advs.201900834
135. Ben S, Yao J, Ning Y, et al. A bioinspired magnetic responsive cilia array surface for microspheres underwater directional transport. *Sci China Chem.* 2020;63(3):347–353. Available at: https://doi.org/10.1007/s11426-019-9660-5
136. Kravanja G, Kriegl R, Hribar L, et al. Magnetically Actuated Surface Microstructures for Efficient Transport and Tunable Separation of Droplets and Solids. *Adv Eng Mater.* 2023;25(22):2301000. Available at: https://doi.org/10.1002/adem.202301000
137. Shao K, Jiang S, Hu Y, et al. Bioinspired Lubricated Slippery Magnetic Responsive Microplate Array for High Performance Multi-Substance Transport. *Adv Funct Mater.* 2022;32(40):2205831. Available at: https://doi.org/10.1002/adfm.202205831
138. An H, Jia N, Wang S, Peng Z, Chen S. Enhanced self-cleaning performance of bio-inspired micropillar-arrayed surface by shear. *Bioinspir Biomim.* 2022;17(6):066005. Available at: https://doi.org/10.1088/1748-3190/ac877b
139. Li J, Su K, Liu H, Zou Y. Recent Advances in Magnetically Actuated Droplet Manipulation for Biomedical Applications. *Magnetochemistry.* 2024;10(4):28. Available at: https://doi.org/10.3390/magnetochemistry10040028
140. Zhou Z, Liu T, Gu X, Zhu Z, Cheng Q, Jiang H. Bidirectional Object Transport on Biomimetic Setal Array with Friction Anisotropy. *Tribol Lett.* 2025;73(2):56. Available at: https://doi.org/10.1007/s11249-025-01993-2
141. Cheng Q, Yang F, Jiang H, Cai H. Investigation of the friction reduction and anisotropy of seta structure with large deflection cantilever beam model. *Tribol Int.* 2022;172:107640. Available at: https://doi.org/10.1016/j.triboint.2022.107640
142. Cheng Q, Yang F, Yang Z, et al. Friction Reduction and Motion Stability of Setal Array Sliding on Rough Surface. *Tribol Lett.* 2023;71(4):114. Available at: https://doi.org/10.1007/s11249-023-01784-7
143. Cheng Q, Yang F, Zhou Z, et al. Research on the friction regulation of biomimetic multi-layer setal arrays under cooperative deformation effects. *Friction.* 2025:9441134. Available at: https://doi.org/10.26599/FRICT.2025.9441134
144. Gupta J, Gupta R, Vanshita. Microneedle Technology: An Insight into Recent Advancements and Future Trends in Drug and Vaccine Delivery. *Assay Drug Dev Technol.* 2021;19(2):97–114. Available at: https://doi.org/10.1089/adt.2020.1022
145. Nguyen HX, Nguyen CN. Microneedle-Mediated Transdermal Delivery of Biopharmaceuticals. *Pharmaceutics.* 2023;15(1):277. Available at: https://doi.org/10.3390/pharmaceutics15010277
146. Garland MJ, Migalska K, Mahmood TMT, Singh TRR, Woolfson AD, Donnelly RF. Microneedle arrays as medical devices for enhanced transdermal drug delivery. *Expert Rev Med Devices.* 2011;8(4):459–482. Available at: https://doi.org/10.1586/erd.11.20
147. McKenna PE, Abbate MTA, Vora LK, et al. Polymeric Microarray Patches for Enhanced Transdermal Delivery of the Poorly Soluble Drug Olanzapine. *ACS Appl Mater Interfaces.* 2023;15(26):31300–31319. Available at: https://doi.org/10.1021/acsami.3c05553
148. Liu G, Yang J, Zhang K, et al. Recent progress on the development of bioinspired surfaces with high aspect ratio microarray structures: From fabrication to applications. *J Controlled Release.* 2024;367:441–469. Available at: https://doi.org/10.1016/j.jconrel.2024.01.054
149. Zhu Z, Wang J, Pei X, et al. Blue-ringed octopus-inspired microneedle patch for robust tissue surface adhesion and active injection drug delivery. *Sci Adv.* 2023;9(25):eadh2213. Available at:

https://doi.org/10.1126/sciadv.adh2213
150. Bok M, Zhao ZJ, Hwang SH, et al. Biocompatible All-in-One Adhesive Needle-Free Cup Patch for Enhancing Transdermal Drug Delivery. *ACS Appl Mater Interfaces.* 2021;13(48):58220–58228. Available at: https://doi.org/10.1021/acsami.1c18750
151. Chen MC, Huang SF, Lai KY, Ling MH. Fully embeddable chitosan microneedles as a sustained release depot for intradermal vaccination. *Biomaterials.* 2013;34(12):3077–3086. Available at: https://doi.org/10.1016/j.biomaterials.2012.12.041
152. Song M, Park HK, Kim M, et al. Skin-adaptive nanofiber-based adhesive electronics with octopus-like 3D suction cups for enhanced transdermal delivery. *npj Flex Electron.* 2025;9:54. Available at: https://doi.org/10.1038/s41528-025-00433-4
153. Brubaker CE, Messersmith PB. Enzymatically Degradable Mussel-Inspired Adhesive Hydrogel. *Biomacromolecules.* 2011;12(12):4326–4334. Available at: https://doi.org/10.1021/bm201261d
154. Wang P, Liu M, Sun J, et al. 4D-printable photocurable pressure sensitive adhesives derived from waste cooking oil. *Virtual Phys Prototyp.* 2025;20(1):e2499490. Available at: https://doi.org/10.1080/17452759.2025.2499490